



Licentiate Thesis in Structural Engineering and Bridges

Reliability-Based Assessment and Optimization of High-Speed Railway Bridges

REZA ALLAHVIRDIZADEH

Reliability-Based Assessment and Optimization of High-Speed Railway Bridges

REZA ALLAHVIRDIZADEH

Academic Dissertation which, with due permission of the KTH Royal Institute of Technology, is submitted for public defence for the Degree of Licentiate of Engineering on Friday the 1st October 2021, at 1:00 p.m. in M108, Brinellvägen 23, Stockholm.

Licentiate Thesis in Structural Engineering and Bridges
KTH Royal Institute of Technology
Stockholm, Sweden 2021

© REZA ALLAHVIRDIZADEH

ISBN 978-91-7873-977-6

TRITA-ABE-DLT-2133

Printed by: Universitetsservice US-AB, Sweden 2021

Abstract

Increasing the operational speed of trains has attracted a lot of interest in the last decades and has brought new challenges, especially in terms of infrastructure design methodology, as it may induce excessive vibrations. Such demands can damage bridges, which in turn increases maintenance costs, endangers the safety of passing trains and disrupts passenger comfort. Conventional design provisions should therefore be evaluated in the light of modern concerns; nevertheless, several previous studies have highlighted some of their shortcomings. It should be emphasized that most of these studies have neglected the uncertainties involved, which prevents the reported results from representing a complete picture of the problem. In this respect, the present thesis is dedicated to evaluating the performance of conventional design methods, especially those related to running safety and passenger comfort, using probabilistic approaches. To achieve this objective, a preliminary study was carried out using the first-order reliability method for short/medium span bridges passed by trains at a wide range of operating speeds. Comparison of these results with the corresponding deterministic responses showed that applying a constant safety factor to the running safety threshold does not guarantee that the safety index will be identical for all bridges. It also shows that the conventional design approaches result in failure probabilities that are higher than the target values. This conclusion highlights the need to update the design methodology for running safety. However, it would be essential to determine whether running safety is the predominant design criterion before conducting further analysis. Therefore, a stochastic comparison between this criterion and passenger comfort was performed. Due to the significant computational cost of such investigations, subset simulation and crude Monte-Carlo (MC) simulation using meta-models based on polynomial chaos expansion were employed. Both methods were found to perform well, with running safety almost always dominating the passenger comfort limit state. Subsequently, classification-based meta-models, e.g. support vector machines, k -nearest neighbours and decision trees, were combined using ensemble techniques to investigate the influence of soil-structure interaction on the evaluated reliability of running safety. The obtained results showed a significant influence, highlighting the need for detailed investigations in further studies. Finally, a reliability-based design optimization was conducted to update the conventional design method of running safety by proposing minimum requirements for the mass per length and moment of inertia of bridges. It is worth mentioning that the inner loop of the method was solved by a crude MC simulation using adaptively trained Kriging meta-models.

Keywords: High-speed railway bridges; Bridge dynamics; Running safety; Passenger comfort; Structural reliability; Meta-models; Surrogate models; Adaptive sampling; Reliability-based design optimization.

Sammanfattning

Att öka tågens hastighet har väckt stort intresse under de senaste decennierna och har medfört nya utmaningar, särskilt när det gäller broanalyser, eftersom tågen inducerar stora vibrationer. Sådana vibrationer kan öka underhållskostnaderna, äventyra säkerheten för förbipasserande tåg och påverka passagerarkomforten. Konstruktionsbestämmelser bör därför utvärderas mot bakgrund av dessa problem; dock har flera tidigare studier belyst några av bristerna i dagens bestämmelser. Det bör understrykas att de flesta av dessa studier har försummat de osäkerheter som är involverade, vilket hindrar de rapporterade resultaten från att representera en fullständig bild av problemet. I detta avseende syftar denna avhandling till att utvärdera prestandan hos konventionella analysmetoder, särskilt de som rör körsäkerhet och passagerarkomfort, med hjälp av sannolikhetsmetoder. För att uppnå detta mål genomfördes en preliminär studie med första ordningens tillförlitlighetsmetod för broar med kort/medellång spännvidd som passeras av tåg med ett brett hastighetsspektrum. Jämförelse av dessa resultat med motsvarande deterministiska respons visade att tillämpa en konstant säkerhetsfaktor för verifieringen av trafiksäkerhet inte garanterar att säkerhetsindexet kommer att vara identiskt för alla broar. Det visar också att de konventionella analysmetoderna resulterar i brottsannolikheter som är högre än målvärdena. Denna slutsats belyser behovet av att uppdatera analysmetoden för trafiksäkerhet. Det skulle emellertid vara viktigt att avgöra om trafiksäkerhet är det dominerande designkriteriet innan ytterligare analyser genomförs. Därför utfördes en stokastisk jämförelse mellan detta kriterium och kriteriet för passagerarkomfort. På grund av den betydande analys tiden för sådana beräkningar användes delmängdssimulering och Monte-Carlo (MC) simulering med metamodeller baserade på polynomisk kaosutvidgning. Båda metoderna visade sig fungera bra, med trafiksäkerhet som nästan alltid dominerade över gränsningstillståndet för passagerarkomfort. Därefter kombinerades klassificeringsbaserade metamodeller som stödvektormaskin och beslutsträd genom ensembletekniker, för att undersöka påverkan av jord-brointeraktion på den utvärderade tillförlitligheten gällande trafiksäkerhet. De erhållna resultaten visade en signifikant påverkan och betonade behovet av detaljerade undersökningar genom ytterligare studier. Slutligen genomfördes en tillförlitlighetsbaserad konstruktionsoptimering för att föreslå ett minimikrav på erforderlig bromassa per längdmeter och tröghetsmoment. Det är värt att nämna att metodens inre loop löstes med en MC-simulering med adaptivt tränade Kriging-metamodeller.

Nyckelord: Høghastighetsjárnsvägsbroar; Brodynamik; Trafiksäkerhet; Passagerarkomfort; Konstruktioners tillförlitlighet; Metamodeller; Surrogatmodeller; Adaptiv sampling; Tillförlitlighetsbaserad designoptimering.

Preface

The research presented in this thesis was conducted at the Department of Civil and Architectural Engineering, KTH Royal Institute of Technology, Stockholm. It was gratefully supported by the In2Track2 project, which is part of the Shift2Rail joint undertaking under the research and innovation program of European Unions Horizon 2020, under grant agreement No. 826255.

I would like to express my sincere gratitude to my supervisors Professor Raid Karoumi and Dr. Andreas Andersson for their professional guidance, valuable support and trust in me during the last years. I am very grateful for everything I have learned from them, and also for their kind respect for my ideas, even if most of them seem strange. A special thanks to Professor John Leander for taking the time to review this work and provide valuable comments, and to Professor Daniel Straub for agreeing to read the work and lead the discussions during the licentiate seminar. I also thank all my friends and colleagues in the Division of Structural Engineering and Bridges and those from other divisions for all the moments we spent together.

Last but not least, I would like to dedicate this work to my wife Negar and my parents Parvin and Moharram for their unconditional love. The probability of me failing due to the unbearable lightness of life without being among them and receiving all their support would be almost one.

Stockholm, August 2021
Reza Allahvirdizadeh

Publications

The current thesis is based on the outcomes presented in the following publications, labelled **Paper I–IV**.

Paper I	Allahvirdizadeh, R., Andersson, A. and Karoumi, R. "Reliability assessment of the dynamic behavior of high-speed railway bridges using first order reliability method". <i>EURODYN 2020, XI International Conference on Structural Dynamics</i> .
Paper II	Allahvirdizadeh, R., Andersson, A. and Karoumi, R. "Surrogate-assisted versus subset simulation-based stochastic comparison between running safety and passenger comfort design criteria of high-speed railway bridges". <i>ESREL 2021, the 31th European Safety and Reliability Conference</i> .
Paper III	Allahvirdizadeh, R., Andersson, A. and Karoumi, R. "Ensemble meta-models for running safety assessment of high-speed railway bridges considering soil-structure interaction effects". <i>ICOSSAR 2021, the 13th International Conference on Structural Safety and Reliability</i> .
Paper IV	Allahvirdizadeh, R., Andersson, A. and Karoumi, R. "Minimum design requirements of high-speed railway bridges using reliability-based optimization". Submitted for review in <i>Journal of Probabilistic Engineering Mechanics</i> .

All papers were planned, implemented and written by Reza Allahvirdizadeh. The co-authors contributed to the papers with comments and revisions.

In addition to the abovementioned papers, the author has contributed to the following related publication:

- Andersson, A., **Allahvirdizadeh, R.**, Zangeneh, A., Silva, A., Ribeiro, D., Ferreira, G. and Montenegro, P. "High-speed low cost bridges: background report for In2Track2", 2021.

Contents

Preface	v
Publications	vii
1 Introduction	1
1.1 State of the art	7
1.2 Aims and scope	9
1.3 Scientific contribution	11
1.4 Outline of the thesis	12
2 Reliability Analysis and Reliability-Based Design Optimization	15
2.1 First order reliability method	16
2.2 Simulation-based methods	22
2.3 Reliability-based design optimization	33
3 Meta-modelling	39
3.1 Adaptive enrichment	41
3.2 Ensemble models	44
3.3 Gaussian process (Kriging)	45
3.4 Polynomial chaos expansion (PCE)	49
3.5 Support vector machines (SVM)	53
3.6 K-Nearest Neighbours (k-NN)	56
3.7 Decision Tree	57
4 Summary of appended papers	61
5 Concluding remarks	69
5.1 Discussion	69
5.2 Conclusions	70
5.3 Further research	70
References	73
Paper I	85
Paper II	101
Paper III	111
Paper IV	125

Chapter 1

Introduction

Increasing transportation demands along with stricter sustainability regulations have directed many interests to rail-based options. This is especially true for the substitution of short- and medium-distance airborne journeys with high-speed trains. An exemplary empirical study has shown such benefits for the London-Paris route, suggesting that similar conclusions can be derived for other conditions (Givoni, 2007). As a result, strategic plans have been developed worldwide to increase the operating speeds of existing lines or to build new high-speed lines. For instance, the share of high-speed lines in total railways in China increased from almost 0.8% in 2008 to nearly 16.4% in 2015 (Hailin et al., 2017). In Europe, the same plan has been developed aiming at tripling the network with an approximate length of 10,000 km in 2010 within a period of 20 years until 2030 (European Commission. Directorate General for Mobility, 2010). It is obvious that trains with higher speeds and/or heavier axle loads induce greater demands on infrastructure, especially bridges. Therefore, our understanding about their dynamic behaviour needs to be updated and new challenges should be addressed, one of which is the resonance condition.

The phenomenon of resonance occurs when the loading frequency is equal to the fundamental frequency of the bridge (or an integer multiple of it). Therefore, the resonant speed (critical speed) can be calculated as (Frýba, 2001; Xia et al., 2006):

$$v_{n,j} = \frac{f_n D}{j} \quad j = 1, 2, 3, \dots, 1/2, 1/3, 1/4, \dots \quad (1.1)$$

where, f_n is the n th natural frequency of the bridge and D is the characteristic axle distance.

This situation was not a problem on older railway lines, but with the increasing speed of trains it has become one of the main problems on modern infrastructures. These excessive vibrations may violate *running safety* due to the loss of contact between the wheel and the rail or the destabilisation of the ballast, disturb the *passenger comfort*, increase the possibility of fatigue occurrence and crack initiation/propagation. The present study is devoted to the investigation of running safety and passenger comfort limit states.

It is worth mentioning that ballast instability occurs when the induced inertial forces on the particles due to their vertical acceleration exceed the resistive forces

CHAPTER 1. INTRODUCTION

such as their weight, interlocking or friction. Therefore, it is implicitly controlled by limiting the vertical acceleration of the bridge deck. This premise is justified by conducted shaking table experiments, where it was shown that particles initiate to displace at vertical accelerations beyond 7.0 m/s^2 (Zacher and Baessler, 2005). Similar conclusions can also be derived from (Kumakura et al., 2010; Nakamura et al., 2011). For the design objectives, a safety factor of 2.0 is assumed in CEN (2003b). It should be emphasised here that, to the author's knowledge, no verification exists for this recommendation.

A general schematic representation of the various aspects involved in the analysis of the dynamic behaviour of railway bridges is shown in Figure 1.1. As it is shown the problem of investigating the dynamic response of bridges due to passing trains is a combination of four general subdivisions including the bridge structure, properties of the track, characteristics of the passing train and the boundary conditions at the site. The earlier studies on this subject modelled the problem either as the motion of a massless force (Ayre et al., 1950; Chen, 1978; Dugush and Eisenberger, 2002; Gbadeyan and Oni, 1995; Jeffcott, 1929; Rao, 2000; Sridharan and AK, 1979; Timoshenko, 1922; Vellozzi, 1967; Wang, 1997; Wu and Dai, 1987; Zheng et al., 1998) or lumped mass (with or without consideration of suspension system - the former is called *sprung mass*) (Akin and Mofid, 1989; Hillerborg, 1951; Sadiku and Leipholz, 1987; Stanišić, 1985; Stanišić and Hardin, 1969; Stokes, 1849; Ting et al., 1974) over a simply-supported beam. Other classical studies in which the interested reader can follow evolutions in this field are Biggs (1964); Frýba (1996, 2013); Garg and Dukkipati (1984); Timoshenko and Young (1955). In general, these simplified approaches neglect train-track-bridge interaction (TTBI) and the effects of boundary conditions (soil-structure interaction - SSI).

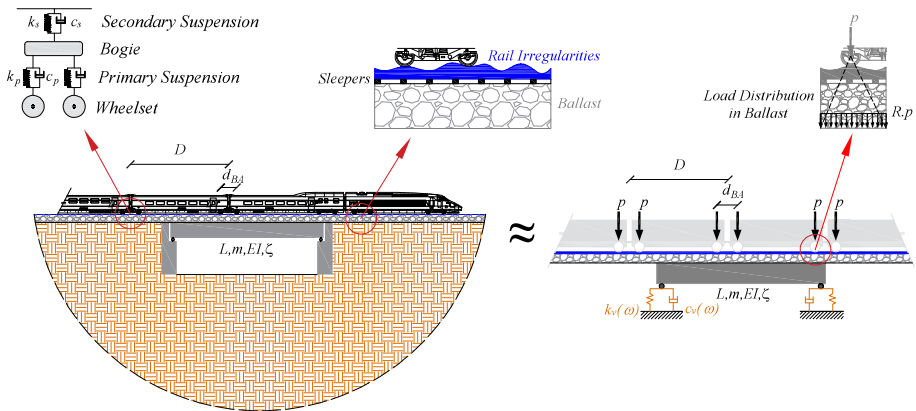


Figure 1.1: Schematic view of modelling the dynamic behaviour of bridges due to train passage.

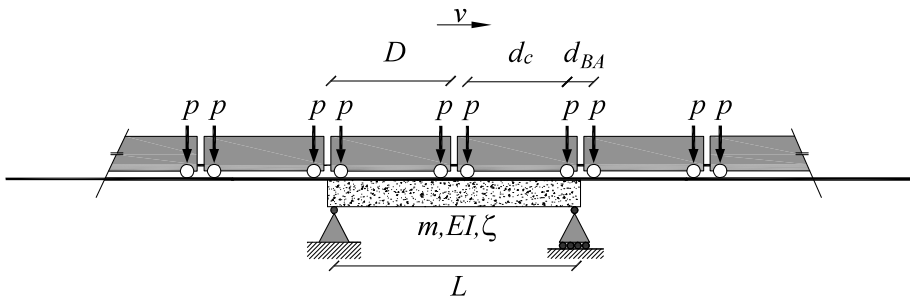


Figure 1.2: Equidistant series of moving loads (articulated train) passing over a simply-supported Euler-Bernoulli beam.

It has been found that the moving force approach can lead to acceptably accurate response predictions when the mass of the train is negligible compared to that of the bridge (Yang and Yau, 1998) and also if the rail is very smooth with no irregularities. Therefore, they are often used when only the assessment of the dynamic response of the bridge is of interest. In such circumstances, a train can be modelled as a series of moving forces (composition of two equidistant series of loads), neglecting the inertial effects of the coaches as shown in Figure 1.2. Considering this simplification, analytical solutions for simply supported Euler-Bernoulli beams representing the bridge superstructure were developed in Frýba (2001); Yang et al. (2004, 1997). These solutions are obtained by superposition of the previously developed analytical solutions for the single moving force problem. The formulation proposed in Yang et al. (2004) for the deflection of the beam is presented as:

$$u(x, t) = \sum_{n=1}^{\infty} q_n(t) \sin\left(\frac{n\pi x}{L}\right) \quad (1.2)$$

$$q_n(t) = \frac{2pL^3}{EI\pi^4} \left[F_n(v, t) + F_n(v, t - d_c/v) \right] \quad (1.3)$$

$$F_n(v, t) = \frac{1}{n^4} \sum_{j=1}^N \frac{1}{(1 - S_n)^2 + (2\xi_n S_n)^2} \left[A(t - t_j) H(t - t_j) + (-1)^{n+1} A(t - t_j - L/v) H(t - t_j - L/v) \right] \quad (1.4)$$

CHAPTER 1. INTRODUCTION

$$A(t) = (1 - S_n^2) \sin \Omega_n t - 2\xi_n S_n \cos \Omega_n t + \exp(-\xi_n \omega_n t) \left[2\xi_n S_n \cos \omega_{dn} t + \frac{S_n}{\sqrt{1 - \xi_n^2}} (2\xi_n^2 + S_n^2 - 1) \sin \omega_{dn} t \right] \quad (1.5)$$

where, $u(x, t)$ is the deflection of the beam at location of x and time of t , N is the number of coaches, $S_n = n\pi v / \omega_n L$ is the speed parameter, $\Omega_n = n\pi v / L$ is the exciting frequency, ξ_n is the modal damping ratio of the n th mode of vibration, $H(\bullet)$ is the Heaviside function, ω_n is the frequency of the n th mode of vibration of the beam and $\omega_{dn} = \omega_n \sqrt{1 - \xi_n^2}$ is the n th damped frequency of vibration.

Significant improvements in computational capabilities have led to the development of advanced models that take into account the interaction between the train and the bridge. Such models allow the response of both subsystems (track-bridge and train) to be evaluated simultaneously; however, they significantly increase the complexity and hence the computational cost of the problem. In this approach, the dynamic response of each subsystem is computed iteratively using the governing equations of motion (see Eq. 1.6) coupled together by *dynamic interaction (contact) force* at their point of contact (Wu, 2000; Yang and Yau, 1998; Zhai et al., 2013). The solution can be obtained by assuming a displacement at the contact point and using the equation of motion of the train to calculate the contact force. Then it is substituted into the equation of motion of the bridge to update the displacement at the contact point (Liu et al., 2014; Yang and Fonder, 1996; Yang et al., 2004). Moreover, it would be possible to solve coupled equations without iterating at each step by accepting larger matrices. The interested reader can find detailed information on this approach in Arvidsson (2018). Using these approaches provides the possibility to implement possible unevenness or imperfections in the rail, known as *rail irregularity*.

$$\begin{cases} \mathbf{M}_{TB} \ddot{\mathbf{u}}_{TB} + \mathbf{C}_{TB} \dot{\mathbf{u}}_{TB} + \mathbf{K}_{TB} \mathbf{u}_{TB} = \mathbf{p}_{TB} \\ \mathbf{M}_V \ddot{\mathbf{u}}_V + \mathbf{C}_V \dot{\mathbf{u}}_V + \mathbf{K}_V \mathbf{u}_V = \mathbf{p}_V \end{cases} \quad (1.6)$$

where, \mathbf{M} , \mathbf{C} and \mathbf{K} are respectively mass, damping and stiffness matrices. \mathbf{u} is the displacement vector and \mathbf{p} is the force vector. Moreover, the indices of TB and V correspond to the track-bridge and vehicle (train), respectively.

In the presence of non-smooth rail at the point of contact, the vertical displacement of the wheel would be equal to the sum of the track-bridge deflection at that point and the rail irregularity (Zhang et al., 2010). The latter is generally modelled as a stochastic Gaussian process (Frýba, 1996), whose mean and autocorrelation functions are obtained using the irregularity profile, which is consequently fitted to the in-situ measurements. This is generally achieved by using the power spectral density (PSD) function describing the amplitude of the track profile at each wavelength (Claus and Schiehlen, 1998).

A comprehensive review of TTBI is given in Arvidsson and Karoumi (2014); Cantero et al. (2016); Zhai et al. (2019). Numerical models were also constructed in Arvidsson and Karoumi (2014) to compare the influence of each modelling strategy on the captured dynamic responses. It was found that considering TTBI can have beneficial effects on vibration reduction; however, these effects may decrease for bridges with larger spans (Museros et al., 2002). Similarly, it was shown in Liu et al. (2009) that the reduction is larger when the mass ratio between the coach and the bridge is larger. Moreover, the difference between the modelling strategy with moving load and the one considering TTBI is most evident in resonance conditions (Arvidsson et al., 2014).

This reduction is implicitly implemented in conventional design guidelines through the *additional damping method* (ADM) (CEN, 2003b; ERRI, 1999), although it has previously been shown to lead to unsafe designs (Arvidsson et al., 2014; Calgaro et al., 2010). Numerical experiments were performed in Arvidsson and Karoumi (2014); Doménech et al. (2014) to distinguish the most influential parameters, where the ratios between bogie-bridge frequency, bogie-bridge mass and coach-bridge length are reported. The same conclusion is reported in Yau et al. (2019), where an analytical approach is presented to consider beneficial influences of TTBI in the moving load modelling strategy. This is called *equivalent additional damping approach* (EADA) and is formulated as:

$$\Delta\xi = \mu_1 r_1 \left| \frac{r_1 + 2\xi_{v1}i}{(1 - r_1)^2 - 2\xi_{v1}r_1i} \right| \approx \mu_1 r_1 \sqrt{r_1^2 + (2\xi_{v1})^2} \quad (1.7)$$

where, μ_1 is the modal mass ratio between the coach and bridge, r_1 is the fundamental frequency ratio of the coach-bridge, and ξ_{v1} is the effective damping ratio of the suspension.

As mentioned earlier, the simplified approaches do not take into account the contribution of the ballast in the load path from the induced axle loads on the superstructure. However, it has been shown for the ballasted tracks that the concentrated axle loads at the rail level are converted into distributed loads at the deck level, which can lead to a significant reduction in bridge response. In numerical simulations, it was observed that the reduction is more remarkable for shorter bridges (Jin et al., 2018). Therefore, reduction coefficients are proposed in ERRI (1999); Jin et al. (2018) to implement such distributions within the track structure implicitly.

Furthermore, SSI effects are typically considered as beneficial parameters because they add damping to the system (NIST, 2012), which leads them to be mostly neglected. However, this view should be taken with caution. This is because taking SSI into account can increase the flexibility of the structure, leading to a shortening of the fundamental frequency (Stewart et al., 1999). The latter means that the critical speed of the bridge would decrease (see Eq. 1.1) (Romero et al., 2013). It is worth mentioning that, due to the non-proportional damping that occurs in

CHAPTER 1. INTRODUCTION

models that take into account SSI effects, a complex eigenvalue problem must be solved in order to obtain modal properties. For this purpose, several toolboxes have been developed, such as *polyeig* (Tisseur and Meerbergen, 2001) and *quadeig* (Hammarling et al., 2013); the former is readily available in MATLAB. Moreover, closed-form expressions have been developed in Zangeneh Kamali et al. (2019) to compute the modal properties of a simple beam resting on viscoelastic supports.

Roughly speaking, shorter span bridges may benefit from the contributions of SSI; however, for longer span bridges, the additional damping may be negligible, resulting in their dynamic behaviour being negatively affected by SSI (Lind Östlund et al., 2020). In this context, it has been shown in previous studies that the consideration of SSI effects (or ground properties at the site) can have a great importance in accurately predicting the vibration of high-speed railway bridges (Takemiya and Bian, 2007; Ülker-Kaustell et al., 2010). In order to introduce SSI effects into the assessment of railway bridges, different modelling strategies are compared in Zangeneh Kamali et al. (2018), where it was shown that simplified approaches using frequency-dependent lumped springs and dashpots can acceptably reproduce the experimentally recorded behaviour. Properly assigning spring and dashpot values requires understanding whether foundation damping would be beneficial or not.

It is shown that the variation between these two scenarios can be distinguished by the ratio of the fundamental frequency of the simply-supported bridge to the fundamental frequency of the soil (as formulated in Eq. 1.8), called *relative frequency parameter*. It has been observed that the damping of the foundation decreases for small values of relative frequency, which becomes negligible for values smaller than 0.5. Therefore, the spring and dashpot parameters can be described by Eqs. 1.9 and 1.10, respectively. On the other hand, for larger values of the relative frequency ($\phi > 1.5$), the behaviour of the system becomes similar to that of the beam resting on a half-space medium. Therefore, the spring and dashpot parameters for this case can be represented by Eqs. 1.11 and 1.12, respectively. In the range of $1 < \phi < 1.5$ (around resonance frequency of the deposit), the damping of the foundation seems to be higher than in the case of resting on a half-space medium. At the same time, the frequency of the systems also shortens more. The assignment of spring and dashpot values in this range requires the construction of more detailed finite element models (Zangeneh Kamali, 2018; Zangeneh Kamali et al., 2019).

$$\phi = \frac{f_{0,ss}}{f_c} = \frac{4Hf_{0,ss}}{V_{La}} = \frac{1.18H\pi(1-\nu_s)f_{0,ss}}{V_s} \quad (1.8)$$

$$k_{st} = \left[\frac{\rho_s V_s^2 A_f}{2B_f(1-\nu_s)} (0.73 + 1.54 \left(\frac{B_f}{L_f} \right)^{3/4} \right] \left(1 + \frac{B_f/H}{0.5 + B_f/L_f} \right) \quad (1.9)$$

$$c_{st} = \frac{\xi_s k_{st}}{\pi f_{0,ss}} \quad (1.10)$$

$$k_{hs} = \left[\frac{\rho_s V_s^2 A_f}{2B_f(1 - \nu_s)} (0.73 + 1.54 \left(\frac{B_f}{L_f} \right)^{3/4}) \right] \quad (1.11)$$

$$c_{hs} = \frac{3.4\rho_s V_s A_f}{\pi(1 - \nu_s)} + \frac{\xi_s k_{hs}}{\pi f_{0,ss}} \quad (1.12)$$

where, $f_{0,ss}$ is the fundamental frequency of the simply-supported bridge, f_c is the frequency of the deposit, H is the depth of stratum, V_{La} is the Lysmer's analog wave velocity (Dobry and Gazetas, 1986), ν_s is the Poisson's ratio of the soil, V_s is the shear wave velocity of the soil, ρ_s is the mass density of the soil, A_f is the area of the foundation, B_f is the semi-width of the foundation, L_f is the semi-length of the foundation, and ξ_s is the damping ratio of the soil material.

1.1 State of the art

Most of the previous studies have investigated various aspects of the dynamic behaviour of railway bridges without considering the uncertainties involved. In this section, a brief overview of the studies that used probabilistic approaches to this topic is presented.

Cho et al. (2010) adopted First-Order Reliability Method (FORM) with limit state functions approximated by polynomial response surfaces. They compared both running safety and passenger comfort limit states, with a larger safety margin given for passenger comfort. The results proposed in this study were obtained by evaluating a bridge subjected to the vibrations of a constant speed train. Therefore, the results presented cannot be extrapolated to derive general conclusions. Similarly, in Rocha et al. (2012), an existing short span reinforced concrete box girder bridge was evaluated to calculate the train speed that satisfies the running safety with prescribed safety margin. They constructed a 2D computational model that considers the interactions between the train and the bridge. A wide range of operational train speeds is considered in this study; however, the induced loads from train passage and the vertical acceleration limit were deterministic (resulting in the method being considered semi-probabilistic). It is worth mentioning that the reliability analyses were carried out using the extreme value theory (tail fitting) with crude Monte-Carlo simulations. Later, the performance of using the Generalized Pareto distribution (GPD) was compared with the sigmoid function in this procedure, both giving acceptably accurate results and significantly reducing the computational cost (Rocha et al., 2014). Moreover, track irregularities were also implemented in their computational model. These authors applied the same methodology to compare the limit states of wheel-rail contact loss and running safety, showing that running safety dominates the design (Rocha et al., 2015, 2016).

CHAPTER 1. INTRODUCTION

Due to the very high computational cost of the crude Monte-Carlo simulation method, a comparison between advanced simulation-based techniques, namely line sampling, subset simulation and asymptotic sampling, was carried out in Hirzinger et al. (2019). In this study, two different bridges were investigated where resonance and track irregularities control their behaviour. It was found that the considered methods can significantly reduce the computational cost without sacrificing accuracy when the track irregularities are neglected. In contrast, their efficiency was decreased in the second model, which has a very large dimensionality (due to the realizations of the track irregularities). Therefore, a detailed study of the influences of random rail irregularities was carried out in Salcher and Adam (2020); Salcher et al. (2019). It was found that a normal distribution can be assigned for the random dynamic deflection of the bridge, while extreme value or lognormal distributions better describe its random acceleration. Based on these observations, stochastic amplification factors were proposed for both deflection and acceleration. It was highlighted that the maximum amplification of deflections due to rail irregularities is about 5%, which may lead to its consideration as a deterministic variable using the codified relationship in Eq. 1.13 (CEN, 2003a) in further studies. However, a significant amplification factor should be expected for accelerations. It has been shown that the codified equation leads to underestimated predictions.

$$\varphi'' = \frac{\alpha}{100} \left[56e^{-(L/10)^2} + 50 \left(\frac{Lf_0}{80} - 1 \right) e^{-(L/20)^2} \right] \quad (1.13)$$

$$\alpha = \min(v/22, 1)$$

where, L is the bridge span length, f_0 is the fundamental frequency of the bridge, and v is the train speed. This value should be reduced by 50% for carefully maintained tracks (which seems to be the case for high-speed lines), and the responses should be multiplied by $1 + \varphi''$.

In terms of probabilistic evaluations of railway bridges, several measures, namely failure probabilities for a given train speed (Eq. 1.14), maximum envelope acceleration (Eq. 1.15), envelope of probabilities (Eq. 1.16) and weighted probability (Eq. 1.17) have been introduced in Hirzinger et al. (2020). The weighted probability of failure seems to be the best measure if precise knowledge about the probability density function of the train speed, i.e. $f_V(v)$ was available. Since such information is usually not available, a uniform distribution is assigned in the desired range of train speeds, resulting in a mean probability ($p_{f_{ave}}$). In this case, $p_{f_{max}}$ and $p_{f_{ave}}$ give an upper and lower bound on the actual probability of failure, respectively. A comparison between p_{f_i} , $p_{f_{max}}$ and $p_{f_{ave}}$ is shown in Figure 1.3. It is based on the results obtained in Paper I for bridges with a span length of 30 m.

$$p_{f_i} = P \left[a_{\max}(v_i) \geq a_{\lim} \right] \quad (1.14)$$

$$p_{f_{max}} = P \left[\max_{v_l \leq v \leq v_u} a_{\max}(v) \geq a_{\lim} \right] \quad (1.15)$$

$$p_{f_{env}} = \max_{v_l \leq v \leq v_u} P(a_{\max}(v) \geq a_{\lim}) \quad (1.16)$$

$$P_{f_w} = \int_{v_l}^{v_u} P(a_{\max}(v) \geq a_{\lim}) f_V(v) dv \quad (1.17)$$

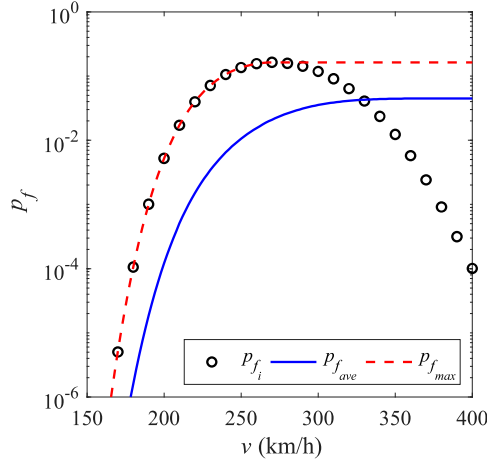


Figure 1.3: Comparison between different probability measures.

1.2 Aims and scope

The overall goal of the study is to first evaluate the reliability of current design guidelines for high-speed railway bridges, particularly running safety, to improve our understanding of them, and then to propose new guidelines if feasible, based on modern objectives. These new guidelines should meet the prescribed safety objectives and it would be much favourable if they could result in lighter bridges.

Conventional design thresholds have been proposed based on limited research, mainly due to restricting computational resources at the time of development. Previous studies have highlighted some of the inconsistencies, deficiencies, or in some cases unacceptable overestimates created by these standards. This licentiate thesis is a first but important step in addressing some of these concerns. In this regard, the focus of this thesis is to consider the uncertainties involved and to apply reliability-

CHAPTER 1. INTRODUCTION

based approaches to evaluate the efficiency of the codified design methods and to update them using reliability-based optimization tools.

Some specific objectives of the thesis are as follows:

- Collect information about contributing variables and assign the corresponding theoretical probability distribution functions using statistical approaches.
- Assess the possibility of potential improvements in current design regulations using simplified reliability-based methods.
- Reviewing advanced simulation-based reliability assessment methods, particularly subset simulation and meta-model assisted approaches (including both regression and classification algorithms such as polynomial chaos expansion, support vector machines, k -nearest neighbours, decision trees and Gaussian process regression) and evaluating their performance with the purpose of reducing the computational costs.
- Application of the discussed advanced methods to discriminate the dominant design criteria (between running safety and passenger comfort) and to investigate the influence of soil-structure interaction on the probability of running safety violation.
- Use reliability-based design optimization to propose minimum allowable mass and stiffness for high-speed railway bridges.

This study is subjected to the following limitations. Only simply-supported single track and single span reinforced concrete bridges are considered. The span length of the considered bridges are in the range of [5-30] m, which represents bridges with short to medium spans. In order to collect information on the geometric characteristics of railway bridges, a limited amount of data was available for high-speed lines. Therefore, some of the information adopted does not necessarily correspond to high-speed lines.

There is no general consensus on whether the running safety limit state corresponds to serviceability or ultimate limit state conditions. Although, the author believes that it is more serviceability concern than the ultimate one. Therefore, target reliability level of $\beta_t = 3.1$ is used in this study.

Due to the limitations of the FORM in the case of nonlinear performance functions, the presented results in Paper I should only be considered for comparison objectives and the absolute values of the safety indices should not be interpreted individually.

1.3. SCIENTIFIC CONTRIBUTION

At this stage of the project, the applicability of the probabilistic approaches and possible improvements to the current rules were of primary interest. Therefore, it was decided to simplify the physical models by considering trains as a series of moving loads. The contribution of train-track-bridge interaction and rail irregularities is implicitly taken into account by equivalent additional damping method and probabilistic amplification factors, respectively; however, it should be admitted that the model (epistemic) uncertainty may increase by applying this approach.

The author was unable to find comprehensive information about resistance-related random variables, i.e. vertical acceleration for running safety and vertical deflection for passenger comfort. The assigned theoretical information for these random variables was obtained based on limited information and judgments of the author. Therefore, they may be subject to higher variation compared to the other variables and are expected to be modified in future studies.

In the Paper III soil-structure interaction effects are considered; however, due to the large uncertainties in soil properties, it was decided to classify them into several groups (rational from the author's point of view) and evaluate the reliability of bridges in these groups. Therefore, presented outcomes are conditioned on the soil properties considered in these groups. In addition, the soil-structure interaction is implicitly modelled by assigning lumped frequency-dependent springs and dashpots at the boundaries of the bridge. Previous deterministic studies have shown that the adopted technique can acceptably predict the dynamic response of railway bridges; however, the author believes that it increases epistemic uncertainties. To implicitly deal with this type of uncertainty, a judgemental random variable (referred to as model uncertainty) is considered. There is no background for this random variable other than the author's judgement and discussion with other experts in the field of railway bridge dynamics.

1.3 Scientific contribution

The research presented in this thesis accompanied by the appended papers, has resulted in the following scientific contributions:

- Distinguishing possible improvements to the conventional design approaches and investigating the sensitivity of the dynamic response with respect to the contributing variables using approximate probabilistic methods (study in Paper I).
- Assignment of appropriate probability distribution functions for basic random variables contributing to the dynamic behaviour of high-speed railway bridges (study in Paper IV).

CHAPTER 1. INTRODUCTION

- Comparison of the performance of meta-model assisted reliability assessment using the Polynomial Chaos Expansion (PCE) surrogate model with the subset simulation method in the context of dynamic problems (study in Paper II).
- Stochastic comparison between running safety and passenger comfort design criteria of high-speed railway bridges to distinguish operational train speeds and spans requiring multiobjective optimization (study in Paper II).
- Evaluating the performance of ensemble meta-models with classification-based heterogeneous models (Support Vector Machines, k -nearest neighbours and Decision Trees) in reliability assessment of railway bridges (study in Paper III).
- Investigating the influence of soil-structure interaction effects on the assessed reliability of high-speed railway bridges (study in Paper III).
- Performing reliability-based design optimization to propose minimum mass and stiffness of high-speed railway bridges that satisfy the desired safety level, assisted by adaptively trained Kriging meta-models (study in Paper IV).

1.4 Outline of the thesis

This thesis is based on four appended papers and mostly presents an extended summary of the concepts discussed in those papers. Chapter 1 reviews the fundamentals of dynamic analysis of railway bridges and previous probabilistic studies on the subject. An overview of applied reliability assessment methods and concepts of reliability-based design optimization are presented in Chapter 2. Chapter 3 discusses meta-modelling concepts including details of the surrogate models used. Chapter 4 summarises the main contents of the appended papers and derived conclusions are presented in Chapter 5. This chapter also includes suggestions for future work.

Paper I employed FORM to perform a computationally inexpensive and preliminary reliability assessment of the running safety of high-speed bridges. FORM method was selected at this time despite its inherent limitations because the objective was to evaluate the safety index for a wide range of operating train speeds (covering both off-resonant and critical speeds) and bridge span lengths (short to medium). It was known from previous studies that conventional design regulations do not prevent violation of running safety by applying unjustified safety factors. Therefore, the resulted safety from the deterministic approach is evaluated approximately to identify possible inconsistencies. Furthermore, the results of the FORM method were used as a sensitivity measure of the evaluated reliability with respect to the considered random variables.

Paper II compares the performance of two advanced simulation-based reliability assessment methods, namely subset simulation and meta-model based Monte-Carlo simulations in dynamic problems. The latter was performed using polynomial chaos expansion as a surrogate model. A set of sensitivity analyses were performed to select the best number of samples and the predefined conditional probability for intermediate events in the subset simulation. Moreover, the leave-one-out cross-validation error was considered to obtain the best configuration of polynomial degrees and truncation scheme of the polynomial chaos expansion method. Their performances were evaluated considering two different performance functions in terms of the running safety and passenger comfort. Moreover, a stochastic comparison between two desired limit states was performed in a wide range of operating train speeds and for bridges with different spans.

Paper III uses the concept of ensemble modelling to train more efficient meta-models. Classification-based models such as support vector machines, k -nearest neighbours and decision trees are used in this study. The main objective of the work was to investigate the influence of soil-structure interaction in the reliability-based evaluation of running safety for high-speed railway bridges. In this context, a simplified modelling technique is used which assigns the spring and the dashpot at boundaries of the bridge. Moreover, due to the large uncertainties in the soil properties, the evaluations are conducted for different classifications. This results in a semi-probabilistic method that gives lower and upper bounds for the probability of failure. These results are given for a wide operating train speeds and bridges with different spans.

Paper IV proposes minimum design requirements, namely mass per length and stiffness (or frequency) for conventional high-speed railway bridges. To achieve this goal, the first part of the study was devoted to collect information on different variables and assigned corresponding probability distribution functions. Then, reliability-based design optimization is performed to obtain the aforementioned values. The violation probability was calculated using a meta-model based Monte-Carlo simulation approach, where Kriging surrogates the computational model. Adaptive sampling techniques are also applied to reduce the computational cost and improve the performance of the meta-models.

Chapter 2

Reliability Analysis and Reliability-Based Design Optimization

Reliability assessment of a structure (either as a system or as a component) includes procedures to ensure its safety with respect to induced actions or to measure the violation probability of limit states. The limit state (interchangeably referred to as performance function or failure surface) is the difference between (or ratio of) resistance (capacity) and actions (e.g., forces, displacements, stresses, or strains); both of which are functions of basic random variables (\mathbf{X}). Therefore, the probability of failure would be evaluated by calculating the reliability integral, which reads as:

$$p_f = P(R - S \leq 0) = P(G(\mathbf{X}) \leq 0) = \int_{\mathcal{D}} f_{\mathbf{X}}(\mathbf{x}) d\mathbf{x} \quad (2.1)$$

where, \mathcal{D} is the failure domain, i.e., the region where $S > R$ and $f_{\mathbf{X}}(x)$ is the joint probability distribution of the basic random variables.

Considering this general definition, the reliability assessment can be performed in the following levels (Madsen et al., 2006):

- **Level I:** is the approach generally taken by regulations, where uncertainties are incorporated into partial safety factors and variables are modelled by their characteristic values.
- **Level II :** uses only the moments (first and second) of random variables together with their correlation coefficients. The exact probability distribution of each random variable or their joint distribution is unknown and they are implicitly considered as Normally distributed.
- **Level III :** uses the joint probability distribution functions to calculate the reliability integral.
- **Level IV :** considers the consequences of the occurrence of a failure (e.g., monetary or fatality). This approach is known as a risk-based method.

CHAPTER 2. RELIABILITY ANALYSIS AND RELIABILITY-BASED DESIGN OPTIMIZATION

In this study, the level II and III approaches are employed. Therefore, a brief description of both approaches is given in this chapter.

2.1 First order reliability method

It is obvious that the calculation of the reliability integral in Eq. 2.1 does not follow a straightforward approach, not only because of the computational cost, but also because of the available information. For example, in most practical cases, the joint probability distribution is not defined. Therefore, some approximate solutions have been developed to provide an estimate of the violation probability (i.e., the nominal probability). Among them, the First order reliability method (FORM) is one of the most commonly used. The fundamental idea of the FORM is to transform the joint probability distribution function in the reliability integral into a multivariate Normal distribution whose solution is readily available. It is worth noting that a brief description of the method is presented here and the interested reader is referred to Melchers and Beck (2018); Nowak and Collins (2012); Sørensen (2011) for more details.

Basic FORM is a Level II reliability assessment method that requires only the expected value (mean) and standard deviation of basic random variables. It also assumes that they are all independent Normal random variables. The other key assumption of FORM is that the limit state function is linear. Considering the limit state function as Eq. 2.2 causes the joint probability distribution function to follow a Normal distribution whose parameters can be easily calculated from the linear combination of the parameters of the basic random variables (see Eq. 2.3). Thus, the reliability integral reduces to the calculation of the standard Normal distribution as Eq. 2.4.

$$G(\mathbf{X}) = \sum_{i=0}^n a_i X_i \quad (2.2)$$

$$f_{\mathbf{X}}(x) \sim \mathcal{N}(\mu_f, \sigma_f) = \mathcal{N}\left(\sum_{i=0}^n a_i \mu_{X_i}, \left(\sum_{i=0}^n a_i^2 \sigma_{X_i}^2\right)^{1/2}\right) \quad (2.3)$$

$$p_f = P(G(\mathbf{X}) \leq 0) = \Phi\left(\frac{0 - \mu_f}{\sigma_f}\right) = \Phi(-\beta) \quad (2.4)$$

where, β is denoted as *safety (reliability) index* (Cornell, 1969). From a geometric point of view, it can be interpreted as the shortest distance from the point with the largest likelihood on the joint probability distribution to the limit state function. Therefore, it can be used as a safety measure where the probability of failure decreases with increasing distance.

It has been shown that the safety index in the original space of basic random variables can vary depending on the definition of the limit state function (e.g., as

2.1. FIRST ORDER RELIABILITY METHOD

a subtraction or ratio). This situation contradicts the goal of being invariant for a safety measure. Therefore, the Hasofer-Lind transformation (Hasofer and Lind, 1974) is proposed as Eq. 2.5 to transform all random variables into the standard Normal space, where they all have expected value and standard deviation equal to zero and one, respectively. Note that the limit state function is changed from $G(\mathbf{X})$ to $g(\mathbf{Y})$. A pictorial example of this transformation is shown in Figure 2.1.

$$Y_i = \frac{X_i - \mu_{X_i}}{\sigma_{X_i}} \quad (2.5)$$

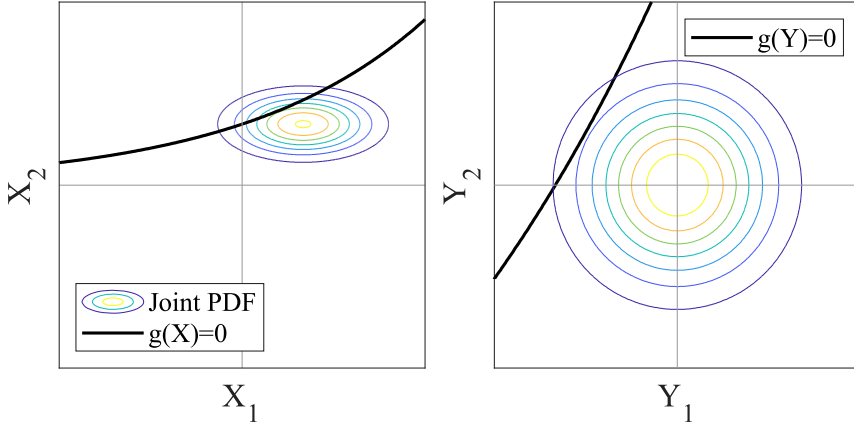


Figure 2.1: Hasofer-Lind transformation.

Then the safety index would be the shortest distance from the origin to the performance function. Therefore, FORM can be reformulated as an optimization problem with quadratic objective function and linear constraint, which is presented in Eq. 2.6. Therefore, optimization toolboxes of programming software such as *Sequential Quadratic Programming* (SQP) of MATLAB can be used for this objective.

$$\begin{aligned} \beta &= \min(\mathbf{Y}^\top \mathbf{Y})^{1/2} \\ \text{s.t.} \quad &g(\mathbf{Y}) = 0 \end{aligned} \quad (2.6)$$

It is worth noting that the point on the limit state function satisfying Eq. 2.6 is called *design (checking) point* (\mathbf{Y}^*). Considering the shape of the joint probability distribution function, the design point has the maximum likelihood on the limit state function (also known as *Most Probable Point* - MPP). Therefore, it has the largest contribution to the calculated violation probability. Hence, this point can

CHAPTER 2. RELIABILITY ANALYSIS AND RELIABILITY-BASED DESIGN OPTIMIZATION

be used for reliability-based design optimization objectives, and the procedure to obtain this point based on the given target safety index is known as inverse FORM problem.

As mentioned, FORM was developed assuming a linear limit state function; however, this is usually not the case in practical situations. This problem is solved by linearising the limit state function using first-order Taylor series expansion (see Eq. 2.7). Given the properties of the design point, the approximation around this point will induce the smallest error in the estimated violation probability. However, it is obvious that based on the shape of the limit state, the estimated nominal violation probability may be overestimated (for concave limit state function towards the origin) or underestimated (for convex limit state function towards the origin).

$$\tilde{g}(\mathbf{Y}) \approx g(\mathbf{Y}^*) + \sum_{i=1}^n (Y_i - Y_i^*) \left. \frac{\partial g}{\partial Y_i} \right|_{\mathbf{Y}^*} = g(\mathbf{Y}^*) + \nabla g(\mathbf{Y}^*)^\top (\mathbf{Y} - \mathbf{Y}^*) \quad (2.7)$$

For better illustration, $\partial g / \partial Y_i$ is expressed by g'_i in the following equations. Moreover, $\mathbf{g}'_{\mathbf{Y}}$ represents the vector of partial derivatives with respect to the basic random variables.

Substituting Eq. 2.7 into Eq. 2.4, taking into account the point that \mathbf{Y}^* lies on the limit state function and assuming that all random variables follow the standard Normal distribution, the safety index can be reformulated as:

$$\beta = -\frac{\mu_{g_L}}{\sigma_{g_L}} = -\frac{\sum_{i=1}^n Y_i^* g'_i}{(\sum_{i=1}^n (g'_i)^2 \sigma_{Y_i}^2)^{1/2}} = -\mathbf{Y}^{*\top} \alpha \quad (2.8)$$

where, α is essentially the direction cosine of the hyperplane of the limit state function at the design point. An important application of the direction cosine besides the computation of the safety index is the evaluation of the sensitivity of the measured safety with respect to each basic random variable (see Eq. 2.9). Moreover, *omission sensitivity factor* is defined as the ratio of the safety index when a basic random variable is considered deterministic to the safety index when all variables are stochastic (Madsen, 1988). In the special case where this variable is removed, the omission sensitivity factor would be like Eq. 2.10.

$$\frac{\partial \beta}{\partial Y_i} = \alpha_i \quad (2.9)$$

$$\gamma_i = \frac{\beta_i^f}{\beta} = \frac{1}{\sqrt{1 - \alpha_i^2}} \quad (2.10)$$

Similar to Eq. 2.6, the design point in Eq. 2.8 is unknown. Therefore, an iterative procedure should be followed to converge the design point; however, it should be

2.1. FIRST ORDER RELIABILITY METHOD

noted that the obtained point does not necessarily correspond to the global minimum (like any other optimization procedure). Therefore, it is always recommended to check the results of FORM with higher level reliability assessment methods, such as Monte-Carlo simulations.

Among the basic assumptions of FORM, the linearity of the limit state function is addressed above. In later steps, the possibility to follow other probability distributions and the dependence between the basic random variables should be implemented in the method.

The transformation of a non-normally distributed random variable of X into a standard normally distributed random variable of Y can be achieved by the Normal tail transformation as shown in Eq. 2.11, where p corresponds to the probability content of $X = x_p$ (Ditlevsen, 1981). It is obvious that there are infinite possibilities for the equivalent Normal distribution (values of μ_z and σ_z) of $F_X(x)$ based on the chosen probability content. One of the good candidates would be the probability content corresponding to the design point. This is because it has a high contribution in the calculated violation probability. In other words, only the area under the joint probability distribution in failure domain (or tail probability) is important to accurately evaluate the violation probability. In summary, the parameters of the equivalent Normal distribution can be calculated using the first-order Taylor series expansion around the design point. It is clear that the design point is initially unknown; therefore, this transformation should be repeated at each iteration.

$$F_X(x_p) = p = \Phi\left(\frac{z - \mu_z}{\sigma_z}\right) = \Phi(y) \quad (2.11)$$

$$\sigma_z = \frac{\phi\left[\Phi^{-1}\left[F_X(x_p)\right]\right]}{f_X(x_p)} \quad (2.12)$$

$$\mu_z = x_p - \Phi^{-1}\left[F_X(x_p)\right]\sigma_z \quad (2.13)$$

The other approach may be to transform non-Normal distributions into equivalent Normal distributions with equal mean and q percentile. It is recommended to set q as target reliability for loading variables and complement of target reliability for resistance variables (Ayyub and Haldar, 1984). Furthermore, for highly skewed distributions, it is recommended to consider the mean of the equivalent Normal distribution as equal to the median of the non-Normal distribution. Then, its standard deviation can be obtained using Eq. 2.12.

The Normal tail approximation can be extended to transform dependent random variables into independent standardized normally distributed random variables, which is called the Rosenblatt transformation (Rosenblatt, 1952). This method

CHAPTER 2. RELIABILITY ANALYSIS AND RELIABILITY-BASED DESIGN OPTIMIZATION

uses the conditional cumulative distribution function to express the required cumulative distribution function of each random variable in terms of Eq. 2.11. As it is evident, the joint probability distribution is not available in many situations, which limits its application. Therefore, we do not go into details of the method here.

To the author's knowledge, in practical problems it is hardly possible to have information about the dependence between random variables. In general, linear correlation from statistical data is the only information that exists in this context, although it does not justify the existence of dependence. Therefore, approximate methods are developed to transform correlated random variables into uncorrelated ones, such as Nataf Transformation and the one based on Cholesky decomposition. The former requires transforming the correlation matrix in the original space to that in the standard Normal space. This task requires iteratively solving the covariance integral, where it is previously solved for certain combinations of probability distributions (Liu and Der Kiureghian, 1986). Nevertheless, it should be evaluated for other combinations. Given these limitations, the latter method is used here. It assumes that \mathbf{T} is a linear and orthogonal transformation matrix (i.e. $\mathbf{T}^\top \mathbf{T} = \mathbf{I}$) that transforms correlated random variables of \mathbf{X} into the uncorrelated standardized normally distributed random variables of \mathbf{Y} (see Eq. 2.14). It is worth noting that the covariance matrix of the transformed random variables is equal to the identity matrix. This is because they are uncorrelated and follow the standard Normal distribution. Therefore, it can be shown that $\mathbf{A} = \mathbf{T}^\top$ is a lower triangular matrix obtained by Cholesky decomposition (see Eq. 2.15).

$$\mathbf{Y} = \mathbf{T}\mathbf{X} \quad (2.14)$$

$$\begin{aligned} \mathbf{C}_\mathbf{Y} \equiv \text{cov}(\mathbf{Y}, \mathbf{Y}^\top) &= \text{cov}(\mathbf{T}\mathbf{X}, \mathbf{X}^\top \mathbf{T}^\top) = \mathbf{T} \text{cov}(\mathbf{X}, \mathbf{X}^\top) \mathbf{T}^\top = \mathbf{T} \mathbf{C}_\mathbf{X} \mathbf{T}^\top \\ &\rightarrow \mathbf{C}_\mathbf{X} = \mathbf{T}^\top \mathbf{C}_\mathbf{Y} \mathbf{T} = \mathbf{T}^\top \mathbf{I} \mathbf{T} = \mathbf{A} \mathbf{A}^\top \end{aligned} \quad (2.15)$$

As mentioned earlier, FORM is an iterative procedure. For this objective, the Hasofer-Lind-Rackwitz-Fiessler (HLRF) method is widely used (Rackwitz and Flessler, 1978). It starts by assuming an initial design point and then the next one is obtained by computing the Taylor series expansion around the previous point. This linearised expression is assumed to be equal to zero since it lies on the limit state function. Given these assumptions and Eq. 2.7, the design point at the next iteration would satisfy Eq. 2.16. This algorithm is summarized in Figure 2.2.

$$\mathbf{Y}^{(i+1)*} = -\alpha^{(i)} \left[\beta^{(i)} + \frac{g(\mathbf{Y}^{(i)*})}{(g'_\mathbf{Y}^{(i)\top} \cdot g'_\mathbf{Y}^{(i)})^{1/2}} \right] \quad (2.16)$$

As discussed, FORM suffers from shortcomings resulting from the simplifying assumptions considered, such as the linearisation of the performance function and the consideration of only the first two moments of the random variables. It is obvious

2.1. FIRST ORDER RELIABILITY METHOD

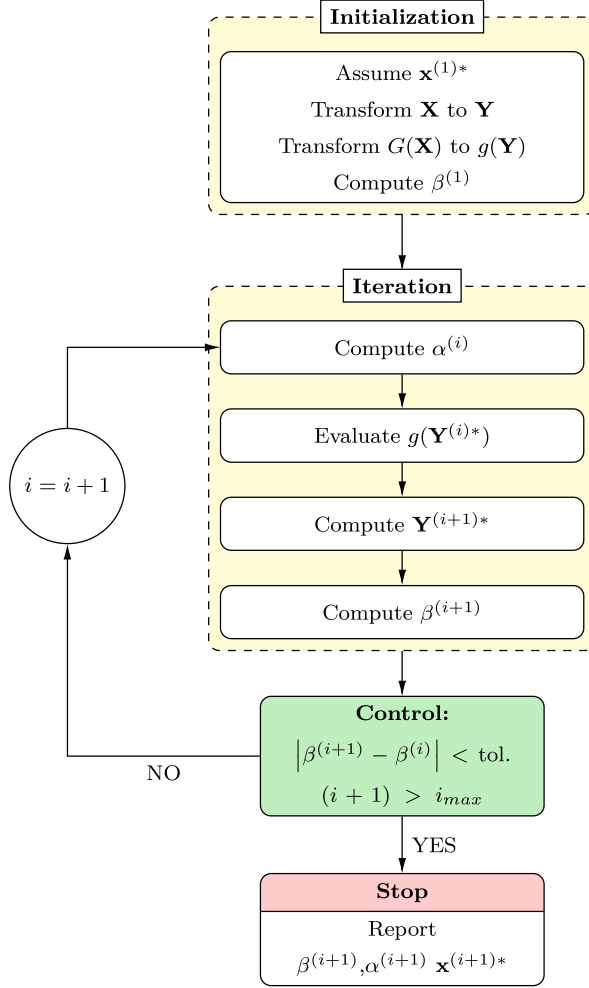


Figure 2.2: The Hasofer-Lind-Rackwitz-Fiessler (HLRF) algorithm.

that the aforementioned limitations may cause FORM not yielding sufficiently accurate results for dynamic problems; however, it can still be used for preliminary investigations or in conjunction with simulation-based approaches. In this context, Paper I investigates whether or not the conventional codified design methods for high-speed railway bridges lead to consistent safety margins.

2.2 Simulation-based methods

As discussed, despite their advantages from a computational point of view, approximate solutions can converge to unreliable predictions, which limits their applicability for complex practical problems. Therefore, simulation-based methods are often used. These methods are basically a numerical integration of the reliability integral in Eq. 2.1 by extensive sampling of basic random variables in their feasible domain (using their corresponding probability density function) and pointwise evaluation of the performance function.

Considering the above idea, Eq. 2.1 can be reformulated as Eq. 2.17 by using an indicator function $\mathbb{I}(\cdot)$ that is equal to one if true and zero otherwise. The reliability problem would then be to compute the expected value of the indicator function in the regions where the performance function is violated. Therefore, evaluating the performance function for each realization of the basic random vector ($\hat{\mathbf{x}}_i$, $i = 1, 2, \dots, N$) and computing the arithmetic mean can result an unbiased predictor of the violation probability. Note that due to the *strong law of large numbers* with $N \rightarrow \infty$, the calculated mean resembles the true violation probability.

$$p_f = \int_{-\infty}^{+\infty} \mathbb{I}[G(\mathbf{X}) \leq 0] f_{\mathbf{X}}(\mathbf{x}) d\mathbf{x} = \mathbb{E} \left[\mathbb{I}[G(\mathbf{X}) \leq 0] \right] \approx \frac{1}{N} \sum_{i=1}^N \mathbb{I}[G(\hat{\mathbf{x}}_i) \leq 0] = \hat{p}_f \quad (2.17)$$

From the *central limit theorem*, it can be concluded that the estimator of the simulation-based method follows a Normal distribution. Furthermore, note that $\mathbb{I}[G(\mathbf{X}) \leq 0]$ follows a Bernoulli distribution that $P \left[\mathbb{I}[G(\mathbf{X}) \leq 0] = 1 \right]$ is equal to p_f . Taking this into account, the coefficient of variation of the above estimator can be used to assess the reliability of the measured violation probability, which reads as:

$$CoV_{\hat{p}_f} = \sqrt{\frac{1 - \hat{p}_f}{\hat{p}_f N}} \quad (2.18)$$

The discussed method is known as *crude Monte-Carlo*. This method is robust; however, it is evident from Eq. 2.18 that the order of its error is inversely related to the number of realizations, i.e., $\mathcal{O}(N^{-1/2})$. Considering the range of violation probabilities in the scope of this study ($10^{-3} - 10^{-4}$), a significant calling number of the computational model (finite element model) is required; which drastically increases the computational cost of the reliability assessment. The situation would be very exhaustive for reliability-based design optimization objectives where many iterations are required to converge to the desired safety level.

To address this issue, several approaches have been developed, such as meta-

modelling, advanced sampling methods, and variance reduction. Meta-models aim to substitute the computational model with an approximate black-box and low-cost model that can compute the desired response in a fraction of the time required by the original model. This approach is taken in Papers II, III and IV. Therefore, the next chapter is devoted to reviewing these methods used here. Then, a brief review of the other approaches is given in the following sections of this chapter.

Example 2.1- FORM versus Crude MC

In this example, the probability of violating the vertical acceleration limit state of a simply-supported Euler-Bernoulli beam with a span length of 20 m subjected to a single moving load passing at a constant speed of 300 km/h is evaluated (see Figure 2.3). In this example, both the FORM and the crude MC methods are used.

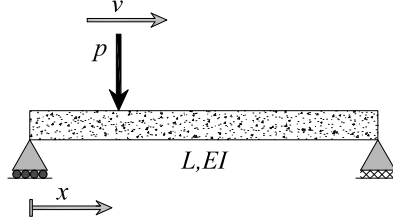


Figure 2.3: Single moving load passing over a simply-supported Euler-Bernoulli beam.

The performance function can be formulated as Eq. 2.19, where the vertical acceleration is calculated using the closed-form solution developed in Yang et al. (2004).

$$\begin{aligned}
 G &= R - S = a_{\text{lim}} - \max |a(x, t)| \\
 a(x, t) &= \frac{2pL^3}{EI\pi^4} \sum_{n=1}^3 \frac{1}{n^4} \sin\left(\frac{n\pi x}{L}\right) \left[\frac{-\Omega_n^2 \sin \Omega_n t + S_n \omega_n^2 \sin \omega_n t}{1 - S_n^2} \right] \\
 \Omega_n &= \frac{n\pi v}{L} \quad S_n = \frac{n\pi v}{\omega_n L} \quad \omega_n = \frac{n^2 \pi^2}{L^2} \sqrt{\frac{EI}{m}} \\
 I &= 0.15 \left(\frac{m}{1000} \right) - 1.2 \quad [m^4]
 \end{aligned} \tag{2.19}$$

All basic random variables are assumed to be independent, and their probability distribution functions are defined in Table 2.1. These values were taken from those given in Paper IV, except for the maximum acceleration threshold which were chosen arbitrarily for illustrative purposes. It is worth

noting that mass per length and moment of inertia are dependent in reality. However, in this example, moment of inertia is considered as a deterministic variable and defined based on a linear regression function fitted to the data collected in the Paper IV (see Eq. 2.19).

Table 2.1: Basic random variables

Variable [unit]	Distribution*	Truncation
a_{lim} [m/s ²]	$\mathcal{N}(2.5, 0.1)$	-
m [kg/m]	$\mathcal{LN}(9.72, 0.26)$	$[400L + 4900, \infty)^\dagger$
p [kN]	$\mathcal{W}(195, 9.1)$	$[120, \infty)$
E [GPa]	$\mathcal{N}(29.7, 3.56)$	-

* \mathcal{N} , \mathcal{LN} and \mathcal{W} correspond to Normal, Lognormal and Weibull distributions, respectively. Parameters of Lognormal distribution correspond to the logarithmic values. Parameters of Weibull distribution correspond to scale and shape.

[†]Truncated based on recommendation of (Museros et al., 2021).

First, the sensitivity of MC with respect to sample size is evaluated in order to select the appropriate sample size. For this purpose, the coefficient of variation (CoV) is calculated as an indicator of its accuracy. Moreover, at each iteration, the safety index is calculated along with its 95% confidence interval. The obtained results are shown in Figure 2.4. As can be seen, the calculated result converges to $\beta = 1.872$ for a sample size larger than 10^5 .

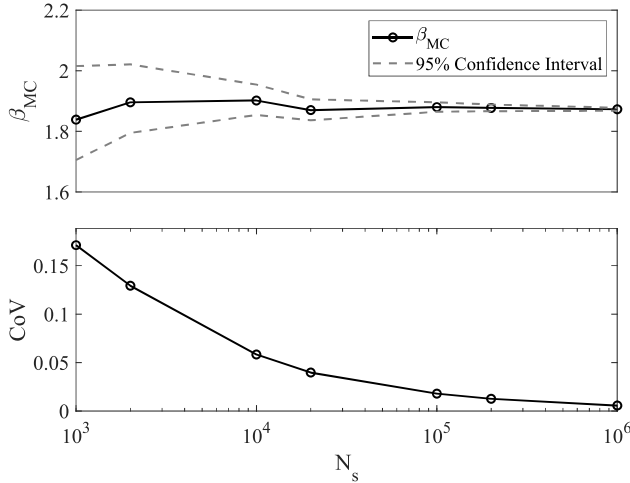


Figure 2.4: Obtained result from crude MC and its performance as a function of sample size.

The comparison between the FORM and the crude MC is shown in Figure 2.5. The FORM resulted in $\beta = 1.876$, which agrees acceptably with the result of MC. To illustrate both methods, the threshold (R) and maximum acceleration (S) are transformed using the Hasofer-Lind transformation (denoted as Z_R and Z_S). The mean and standard deviation were obtained from the generated samples.

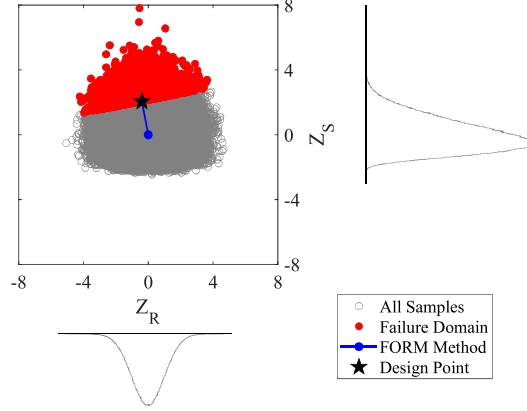


Figure 2.5: Comparison between FORM and crude MC.

The directional cosines obtained by the FORM are shown in Figure 2.6. As discussed earlier, directional cosine values can be used as a sensitivity measure for the calculated safety index with respect to basic random variables. Thus, it can be seen that the mass per length and the load value are the most important variables in this problem.

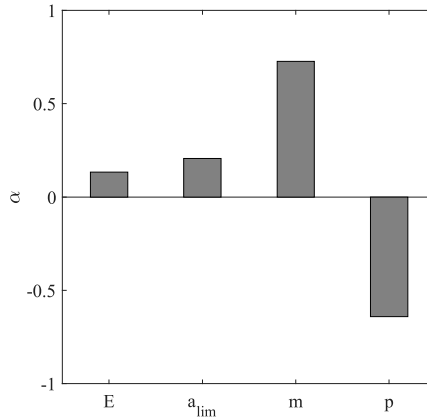


Figure 2.6: Direction cosines from FORM.

2.2.1 Conventional sampling techniques

It is obvious that the number of considered sample points and the procedure for their generation play a key role in simulation-based approaches. Nevertheless, it is substantially important to consider that, despite the designation of the whole procedure of simulation-based reliability assessments as a probabilistic method, it is not possible to generate random numbers from general meaning point of view. In other words, the sequence of numbers is generated according to deterministic approaches, which makes them called *pseudo-random*. Based on Hull and Dobell (1962), a sequence of nonnegative integers can be computed using, for example, the congruence relation in Eq. 2.20.

$$x_i \equiv ax_{i-1} + b \pmod{c} \quad (2.20)$$

where, a , b and c are all integers, with c being much larger than the others. The procedure starts by considering an arbitrary integer x_0 , which is called *seed*. It is obvious that the maximum unique number generated by this method is less than c . Then, one can transform the generated random numbers to the interval $[0, 1)$ by dividing them by c . Afterwards, it would be possible to transform uniformly distributed random numbers with the inverse CDF of the random variable.

This method of sampling gives no control over where each realization would be drawn. Therefore, a significant number of them would be located in regions that do not contribute to the reliability assessment. In this regard, stratified (space-filling) sampling techniques have been developed, among which the *Latin Hypercube* (LHS) is widely used. In this approach, the range of each random variable is partitioned into non-overlapping intervals of equal probability and a sample is drawn from each of these intervals. This method proves to be more efficient than the conventional Monte-Carlo; however, it applies the constraint only to one dimension of the problem. Considering the standard deviation of the minimum distance between sample points as an efficiency indicator of the sampling method, an improved Distributed Hypercube Sampling (IHS) method is proposed in Beachkofski and Grandhi (2002), where the constraint is applied to higher dimensions. This method considers an m -dimensional hypercube around each of N realizations, resulting in the optimal distance between sample points being like Eq. 2.21. It has been shown that this method has a smaller confidence interval than the conventional MC and LHS; however, it is obvious that using this method requires solving an optimization problem.

$$d_{opt} = N^{1-\frac{1}{m}} \quad (2.21)$$

A similar stratified sampling method is proposed based on *Centroidal Voronoi Tessellations* (CVT) (Saka et al., 2007). Voronoi diagrams partition space into convex polytopes where the distance of each point in them to their generator is the smallest with respect to the generators of other polytopes. When the generator of a

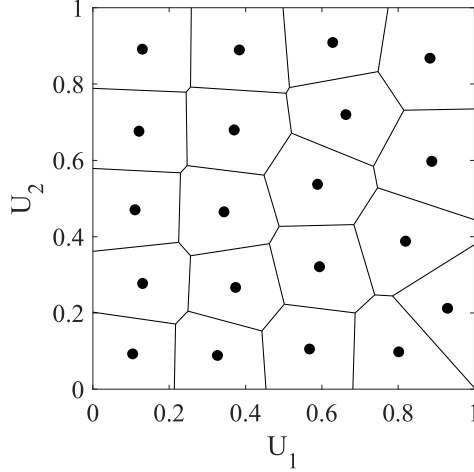


Figure 2.7: Example of Centroidal Voronoi Tessellations (CVT) sampling.

polytope coincides with the mass density of it, it is called a CVT (Burns, 2009). An example of this method is shown in Figure 2.7, where the samples are generated using the CODES toolbox (Missoum et al., 2015). Similar to IHS, it is more efficient than traditional sampling techniques and an optimization problem must be solved to generate these random numbers. Therefore, their performance decreases significantly as the number of required sample points increases and they may suffer from the curse of dimensionality. Therefore, their applicability in experimental design (DOE) seems to be more advantageous for training meta-models. This aspect will be discussed in the next chapter. It is worth noting that the dimensionality of the problem can be reduced using sensitivity analyses. However, such analyses are beyond the scope of the current study.

2.2.2 Copula functions

The methods discussed in the previous section generate independent random numbers, so this section is devoted to generating correlated random numbers. One approach may be to use the inverse method based on the Cholesky decomposition presented in Eq. 2.14, but here the concept of Copula functions is briefly reviewed.

Based on Sklar's theorem, there would be a unique Copula function of C in the n -dimensional domain of the basic random variables X_i , $i = 1, 2, \dots, n$ if the univariate CDFs of all variables are continuous. Then their joint CDF and PDF read as Eqs. 2.22-2.23. It should be noted that the Copula function is an n -variate joint distribution on $[0 - 1]^n$, and from Eq. 2.22 it can be seen that its univariate

CHAPTER 2. RELIABILITY ANALYSIS AND RELIABILITY-BASED DESIGN OPTIMIZATION

marginals are also uniformly distributed as $u_i \sim \mathcal{U}(0, 1)$. In addition, it should be isotonic; that is, $C(\mathbf{X}) \leq C(\mathbf{Y})$ for all $\mathbf{X}, \mathbf{Y} \in [0 - 1]^n$, where $\mathbf{X} \leq \mathbf{Y}$. A variety of Copula families have been proposed in the literature, among which *elliptical* and *Archimedean* ones are the best known. The former typically has no closed-form expression and the number of its parameters is equal to the number of correlation coefficients between random variables. Multivariate Gaussian distribution is one of the widely used elliptical Copula functions; however, it should be noted that it cannot model the dependency between the variables at the tails. On the other hand, Archimedean Copula functions are developed using a generator function, which allows them to be expressed as closed-form expressions and generally have only one defining parameter (Durante and Sempi, 2010).

$$F(X_1, X_2, \dots, X_n) = C(u_1, u_2, \dots, u_n) = C(F_{X_1}(x_1), F_{X_2}(x_2), \dots, F_{X_n}(x_n)) \quad (2.22)$$

$$f(X_1, X_2, \dots, X_n) = \frac{\partial^n C(F_{X_1}(x_1), F_{X_2}(x_2), \dots, F_{X_n}(x_n))}{\partial X_1 \partial X_2 \dots \partial X_n} \prod_{i=1}^n f_{X_i}(x_i) \quad (2.23)$$

This approach is commonly used to generate correlated random numbers for reliability assessment objectives and an example of these compared to independent random numbers is presented in Figure 2.8. The interested reader can find some of its applications in Du et al. (2017); Lu and Zhu (2018); Papaefthymiou and Kurowicka (2008). In this study, the dependency between mass per length and moment of inertia of bridges in Papers II, III and IV is modelled using the Copula concept.

As mentioned earlier, in practical situations the correlation coefficient is usually the only available information about the dependence between random variables. Using it with the concept of maximum likelihood leads to obtain the parameters of the Copula function; however, it is recommended to consider rank-based correlation coefficients rather than conventional linear coefficients (Lu and Zhu, 2018; Papaefthymiou and Kurowicka, 2008). This is because rank-based correlation coefficients remain unchanged under nonlinear transformations.

Moreover, since the true joint distribution between random variables is unknown, it is recommended to select the proper Copula function by computing the Akaike information criterion (AIC) and Bayesian information criterion (BIC) as Eqs. 2.24-2.25 (Akaike, 1974; Schwarz et al., 1978). The first term in these equations represents the difference between the expected value of the true density function when the true density function is used for computation and the case when the log-likelihood of the associated density function is assumed with parameter θ . The second term considers the number of parameters in the definition of the Copula functions. Therefore,

2.2. SIMULATION-BASED METHODS

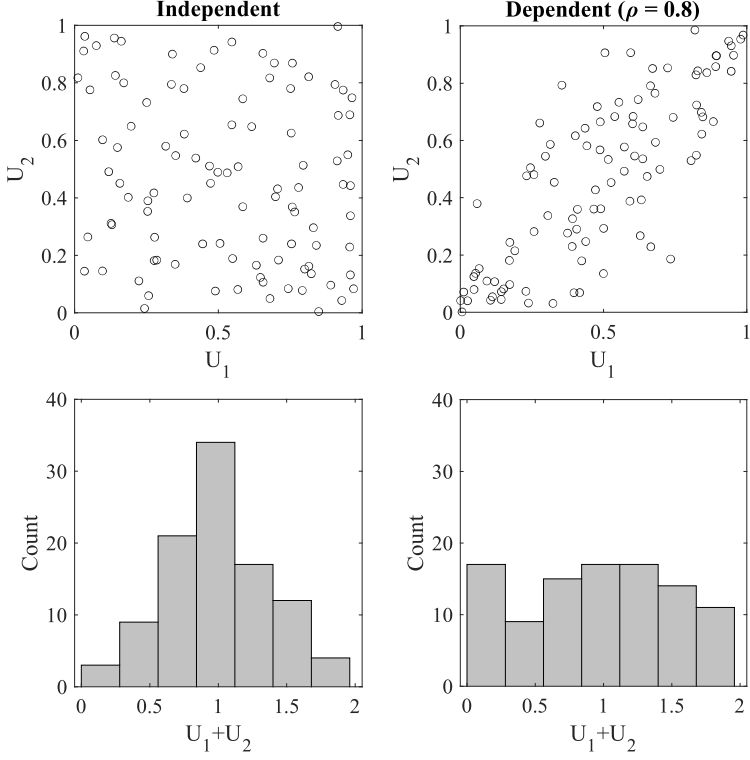


Figure 2.8: Independent versus dependent (using Gaussian copula function) randomly generated samples.

the copula function with minimum AIC and BIC should be used.

$$AIC(\theta) = -2 \sum_{i=1}^N \ln[C(x_i, y_i; \theta)] + 2k \quad (2.24)$$

$$BIC(\theta) = -2 \sum_{i=1}^N \ln[C(x_i, y_i; \theta)] + k \ln(N) \quad (2.25)$$

2.2.3 Variance reduction techniques

Variance reduction methods attempt to improve the performance of the crude Monte-Carlo simulation method by reducing its variance. These methods are not adopted in this study; therefore, only a brief overview of them is presented here.

Important sampling

As mentioned earlier, the majority of the generated samples in the crude Monte-Carlo method would be in the safe domain, resulting in poor performance of the method. On the other hand, it is evident that by taking sample points around the vicinity of the performance function (intersection of load- and resistance-related probability density functions), the chance of generating more advantageous sample points increases. This concept is referred to as *important sampling*. In this case, the generated samples would be drawn using a different function (denoted here as $h_{\mathbf{v}}(\mathbf{x})$ - *instrumental density*) and the reliability integral reads as Eq. 2.26. It has been shown that a carefully chosen important sampling probability density function can reduce the variance of the measured violation probability; however, it should be noted that there is no guarantee of such improvement due to the choice of any function. A good candidate for this may be a multivariate Normal distribution whose mean vector is equal to the design point (obtained from the FORM) and covariance matrix is equal to a diagonal matrix with the variance of the random variables (Kahn, 1956; Melchers, 1984, 1989; Melchers and Beck, 2018; Sørensen, 2011).

$$p_f = \int_{-\infty}^{+\infty} \mathbb{I}[G(\mathbf{X}) \leq 0] \frac{f_{\mathbf{X}}(\mathbf{x})}{h_{\mathbf{v}}(\mathbf{x})} h_{\mathbf{v}}(\mathbf{x}) d\mathbf{x} = \mathbb{E} \left[\mathbb{I}[G(\mathbf{X}) \leq 0] \frac{f_{\mathbf{X}}(\mathbf{x})}{h_{\mathbf{v}}(\mathbf{x})} \right] \quad (2.26)$$

Conditional expectation

According to the *law of total expectation*, for any given random variable Y , the expectation of conditional expected value of the random variable X is equal to the expected value of X (Eq. 2.27). Moreover, it is evident from Eq. 2.28 that the variance of the conditional expected value would be smaller than the variance of the random variable.

$$\mathbb{E}(X) = \mathbb{E}[\mathbb{E}(X|Y)] \quad (2.27)$$

$$\text{Var}(X) = \text{Var}[\mathbb{E}(X|Y)] + \mathbb{E}[\text{Var}(X|Y)] \quad (2.28)$$

Therefore, it would be possible to consider some control variables in the performance function and reformulate the reliability evaluation problem as an expectation of the conditional expectation of the basic random variables given other random variables that can be randomly generated. It is important that the control variables should be statistically uncorrelated with the other basic random variables. Considering X as the control variable and \mathbf{Y} as the vector of the other basic random variables, the violation probability for each realization of \mathbf{Y} , represented as \mathbf{y}_i , is as Eq. 2.29. Then the violation probability would be represented as Eq. 2.30 (Ayyub and Chia, 1992; Ayyub and Haldar, 1984).

$$p_{f_i} = F_X(\mathbf{y}_i) \quad (2.29)$$

$$p_f = \frac{1}{N} \sum_{i=1}^N p_{f_i} \quad (2.30)$$

2.2.4 Subset simulation

The main reason for the poor performance of the crude Monte-Carlo simulation is that it attempts to measure the safety of a rare event (with a very small violation probability). Considering this fact, the subset simulation method is developed, which divides the failure domain into frequent intermediate failure events (with large violation probability). In other words, each intermediate failure event is a subset of higher ones and the union of all of them corresponds to the desired failure domain. Then, it was shown in Au and Beck (2001) that the violation probability can be estimated using Eq. 2.31. It is worth noting that the boundary of the intermediate limit states are adaptively chosen based on the prescribed constant violation probability of each failure event (denoted as p_0). Assuming that N is the number of simulations for each event, the threshold can be chosen as the one in the rank of Np_0 . In summary, the performance of subset simulation would be a function of N and p_0 . Small values of p_0 make the intermediate failure event a rare event and a large value of it requires a large number of subdivisions, both of which reduce the performance of the procedure (Au and Beck, 2001).

$$p_f = P(G_1(\mathbf{X}) < 0) \prod_{i=1}^{m-1} P(G_{i+1}(\mathbf{X}) < 0 | G_i(\mathbf{X}) < 0) = P_{f_1} \prod_{i=1}^{m-1} P_{f_i} \quad (2.31)$$

where, m is the number of intermediate failure events.

The first term of the product can be easily computed using a crude Monte-Carlo simulation with a small number of realizations; however, the others require sampling from the conditional joint probability distribution, which specifies the given violation probability at the previous failure event $f(\mathbf{x}|F_i)$. This is the posterior distribution, which is unknown in the first place. Therefore, it is proposed to sample using the Markov Chain Monte-Carlo (MCMC) with the modified Metropolis-Hastings algorithm (Au and Beck, 2001).

MCMC attempts to sample a sequence of points whose density of final samples is stationary and converges to the posterior with $N \rightarrow \infty$. The Markovian property states that the generation of each sample depends only on the previous sample. Therefore, the samples generated by MCMC cannot be considered as independent and hence the so-called *thinning* procedure can be used to overcome this issue. The latter means selecting a sample at every given t . In this approach, a new sample is proposed based on a proposal distribution (denoted here as $q(\mathbf{x}_{j+1}|\mathbf{x}_j)$); which estimates the probability of generating \mathbf{x}_{j+1} from \mathbf{x}_j and, in the case of subset simulation, is recommended as a uniform distribution centred around the previous

CHAPTER 2. RELIABILITY ANALYSIS AND RELIABILITY-BASED DESIGN OPTIMIZATION

sample and propagating in both directions with length equal to the standard deviation of the random variable (Au and Beck, 2001). The advantage of using such a proposal distribution is its symmetry, i.e. $q(\mathbf{x}_{j+1}|\mathbf{x}_j) = q(\mathbf{x}_j|\mathbf{x}_{j+1})$ (Au and Beck, 2001; Speagle, 2019).

To satisfy the stationarity condition, the *detailed balance* should be valid, i.e., the probability of moving from \mathbf{x}_j to \mathbf{x}_{j+1} ($P(\mathbf{x}_{j+1}|\mathbf{x}_j)$) should be equal to the reverse movement (see Eq. 2.32). The posterior distribution in this equation can be replaced by the obtained probability density from MCMC or, in the case of subset simulation, by the joint probability distribution of the problem. Note that this probability can be computed using the proposal distribution and a transition probability ($T(\mathbf{x}_{j+1}|\mathbf{x}_j) = T_j$) that accepts or rejects this movement (see Eq. 2.33) (Speagle, 2019).

$$P(\mathbf{x}_{j+1}|\mathbf{x}_j)f(\mathbf{x}_j|F_i) = P(\mathbf{x}_j|\mathbf{x}_{j+1})f(\mathbf{x}_{j+1}|F_i) \quad (2.32)$$

$$P(\mathbf{x}_{j+1}|\mathbf{x}_j) = q(\mathbf{x}_{j+1}|\mathbf{x}_j)T(\mathbf{x}_{j+1}|\mathbf{x}_j) \quad (2.33)$$

Considering Eqs. 2.32-2.33 leads to the conclusion that the ratio of the transition probability is equal to the ratio of the posterior distributions multiplied by the ratio of the proposal distribution. Since the proposal distribution is considered symmetric, it can be removed from further calculations.

In summary, to obtain the next sample from the previous one, an initial guess is made and the transition probability is calculated. If this probability is greater than a generated random number with uniform distribution and is a member of the failure domain in the previous intermediate failure event, it would be accepted. Otherwise, the previous point would be considered as a sample in the next state (Au and Beck, 2001; Speagle, 2019). The flowchart of this algorithm is presented in Figure 2.10. It is worth noting that the subset simulation method has been successfully applied to a variety of problems related to structural reliability assessment (Au et al., 2007; Wang, 2020)

Example 2.2- Subset Simulation

In this example, the problem presented in Example 2.1 is again solved using the subset simulation method. It should be emphasised here that these analyses were performed using the toolbox *UQLab* (Marelli and Sudret, 2014). As discussed, the performance of the subset simulation depends on the sample size and the given failure probability of the intermediate events. Therefore, different values for each of these parameters are considered to evaluate the subset simulation performance and select the best parameter configuration. It is worth noting that in the case of varying sample size, the failure

probability of the intermediate events is set to 0.1. Similarly, when the failure probability of intermediate events changes, the sample size is set to 1000. The results are shown in Figure 2.9.

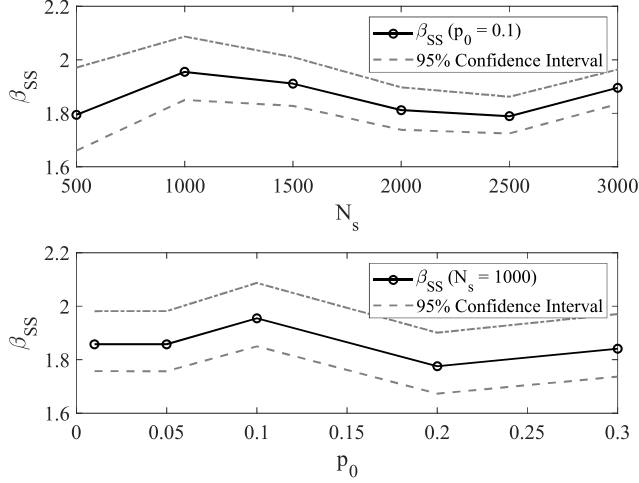


Figure 2.9: Performance of subset simulation as a function of sample size and failure probability of intermediate events.

It can be seen that the default configuration of the subset simulation (i.e. $N_s = 1000$ and $p_0 = 0.1$) leads to $\beta = 1.955$, which presents 4.4% difference with respect to the result of crude MC. This is an acceptable agreement; however, it is evident that a wider confidence interval should be expected from the subset simulation.

Finally, the default configuration of the subset simulation spends less than 5% of the computational cost corresponding to the crude MC.

2.3 Reliability-based design optimization

It is important for any system to fulfill the objectives of its existence, but it is obvious that there is always a trade-off between the gains from its operation and the direct or indirect costs (from a general point of view) paid for its construction or utilization. Dealing with this problem forms the soul of optimization, which is considered a decision-making process. In other words, it looks for the best (optimal) alternative. Traditionally, this problem is considered deterministic, i.e., the optimal solution is sought within a given feasible domain without considering the associated uncertainties. Following this approach may lead to optimal solutions, e.g.,

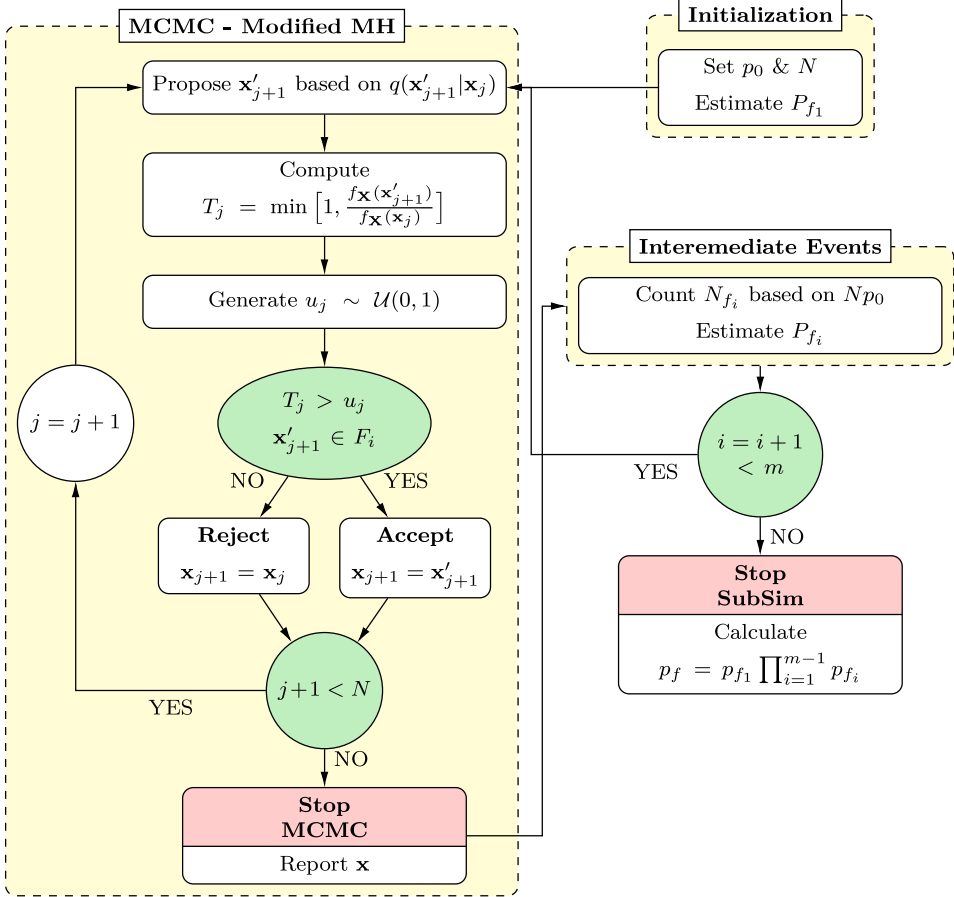


Figure 2.10: The subset simulation algorithm.

minimal masses in structures; however, it was previously shown that this should not be interpreted as being safe also. On the contrary, it has been highlighted that unacceptable failure probabilities can be expected from deterministically optimized structures (Agarwal and Renaud, 2004). For this reason, reliability-based design optimization (RBDO) has been developed, which is believed to be the proper way to solve the above problem. RBDO can be formulated as:

$$\begin{aligned}
 \mathbf{d}^* &= \arg \min_{\mathbf{d} \in \mathcal{D}_d} \mathcal{J}(\mathbf{d}) \\
 \text{s.t. } &\begin{cases} P[G_i(\mathbf{d}, \mathbf{X}) \leq 0] \leq p_{f,i}^{\text{target}} & i = 1, 2, \dots, n_d \\ h_l(\mathbf{d}) \leq 0 & l = 1, 2, \dots, n_h \end{cases}
 \end{aligned} \tag{2.34}$$

2.3. RELIABILITY-BASED DESIGN OPTIMIZATION

where, \mathbf{d} is the vector of design variables, $\mathcal{D}_{\mathbf{d}}$ is the design (feasible) domain, $\mathcal{J}(\bullet)$ is the objective function, $G_i(\mathbf{d}, \mathbf{x})$ is the i th limit state function, $p_{f,i}^{target}$ is the desired safety level, n_d is the number of hard constraints and $h_i(\mathbf{d})$ is the deterministic soft constraint. It is worth noting that some formulations replace the probability-based hard constraints with safety index (β).

It would be useful to formalize the objective function as the total cost of the structure (see Eq. 2.35) or as the total utility function (see Eq. 2.36). Note that the latter should be maximized. Due to difficulties in assigning monetary values, these objective functions are usually replaced by variables related to geometric or physical properties (Enevoldsen and Sørensen, 1994; Frangopol, 1985). Another approach is to normalize the cost function with the initial cost; this removes exact cost values from the procedure, but ultimately requires an engineering judgment for the ratios (Dubourg et al., 2011).

$$C_t = C_0 + C_r + C_f p_f \quad (2.35)$$

$$U_t = B - C_0 - L_f \quad (2.36)$$

where, C_t is the total cost of the structure, C_0 is its initial cost, C_r is the cost of inspection and repair, C_f is the cost of failure, B is the benefit of the structure's existence, and L_f is the expected loss from failure.

Considering the computationally intensive nature of the problem in Eq. 2.34, initial studies led to the use of FORM due to its efficiency. Since FORM is itself an optimization problem; hence, these methods are referred to as *double-loop* or *nested* approaches. The outer loop is the deterministic optimization and the inner loop is the optimization problem of solving the reliability problem.

In a special form, when there is no cost function, *inverse reliability problem* is introduced in Der Kiureghian et al. (1994). This method searches for an unknown parameter on the most probable point (MPP); whose distance from the origin in the standard Normal space is equal to the target reliability index. These methods for solving the reliability problem in RBDO led to propose *reliability index approach* (RIA) and *probabilistic measure approach* (PMA). The interested reader can find their detailed description and also their application in an RBDO example in Ramu et al. (2006).

The aforementioned approaches suffer from two main problems that make their application to practical problems prohibitive. One is the inherent inadequacy of the FORM in the case of highly nonlinear limit state functions and the other is the requirement of calling computational model many times. The computational budget in practical situations is limited; therefore, subsequent revisions of RBDO have been aimed at improving performance from this perspective.

CHAPTER 2. RELIABILITY ANALYSIS AND RELIABILITY-BASED DESIGN OPTIMIZATION

The double-loop problem is reformulated as a *single-loop* problem in Chen et al. (1997). This is achieved by transforming the original space into the reduced space and using the relationship between MPP and safety index. Therefore, solving the costly reliability estimation can be eliminated; however, the method requires the computation of direction cosines on MPP. This is still an iterative procedure and requires invoking a computational model to calculate the derivatives. In another approach, the exact computation of the reliability index is approximated at each step by its first-order Taylor series expansion around MPP; this is known as *sequential approximate programming* (SAP) (Cheng et al., 2006). The examples presented in Cheng et al. (2006) showed a significant improvement with respect to the double- and single-loop methods; however, these methods still require the sensitivities to be calculated using finite difference methods, which subsequently needs calling the computational model. The idea of approximating around the MPP led Agarwal and Renaud (2004) to use the response surface. In their method, called as *second order response surface approximation* (RSA), the difference between the reliability index at this iteration and the target reliability index is approximated by sampling around MPP (Agarwal and Renaud, 2004). Considering the above discussions, the method would not be applicable in complex problems, but the possibility of using meta-models opens a new opportunity in this subject.

In traditional methods for solving RBDO, it was not possible to use simulation-based techniques in the inner loop of the procedure. However, the idea of using meta-models overcomes this issue. Meta-models approximate computational models by functions that are inexpensive to evaluate. This approach is used in much of the current study, so various aspects of this approach are discussed in the next chapter.

In this context, Kriging- or moving-least-square-based meta-models are proposed in Kanakasabai and Dhingra (2014) to surrogate MPP. These meta-models are trained outside the optimization loops with a small experimental design. Then, their efficiency can be improved at each iteration of the optimization. Re-training meta-models at each iteration adds unnecessary cost to the optimization procedure (Dubourg et al., 2011; Moustapha and Sudret, 2019). Therefore, it was recommended to train a sufficiently accurate meta-model outside the procedure. The fundamental idea behind this premise is the point that the meta-model must be very accurate especially around the limit state function. This space is known as the *augmented reliability space*; it can be conceived as a hyper-rectangular where each dimension is equal to the range between the lower and upper bounds of corresponding variable. By this approach, the RBDO procedure is changed into different *non-intrusive* blocks, as shown in Figure 2.11 (Moustapha and Sudret, 2019). This method can solve RBDO problems with very reasonable computational cost, which is adopted in this study.

2.3. RELIABILITY-BASED DESIGN OPTIMIZATION

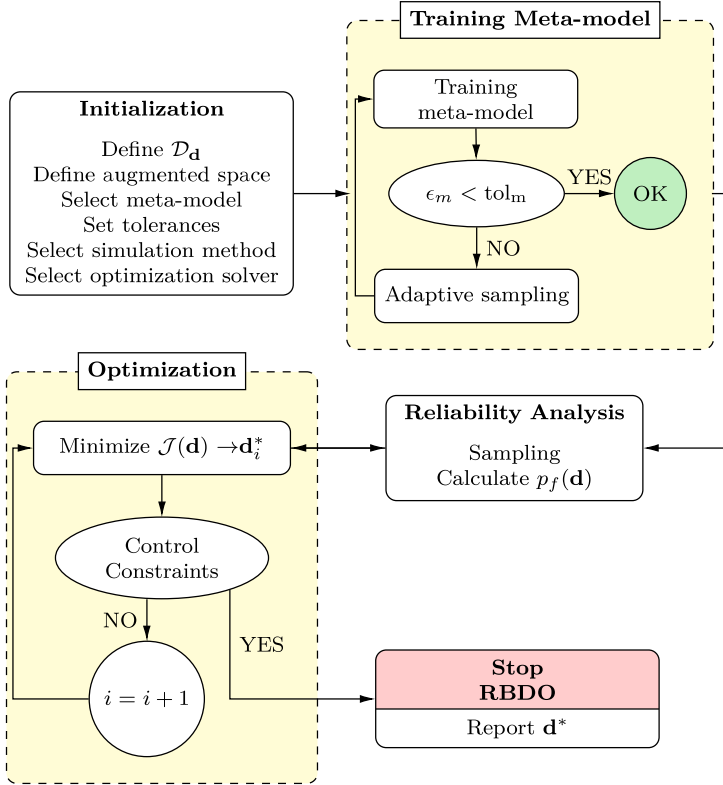


Figure 2.11: The algorithm of the adopted Reliability-Based Design Optimization (RBDO).

Chapter 3

Meta-modelling

As discussed in the previous chapter, the crude Monte-Carlo simulation requires many recalls of the computational model, which makes it prohibitively expensive to use. In addition to the solutions discussed earlier, the introduction of meta-models (*emulator*) which surrogate the computational model (*simulator*) has received a significant attention in the last decade to reduce the computational cost of reliability assessment. Meta-models are interchangeably known as surrogate models and are also traditionally referred to as response surfaces. As stated in Dubourg et al. (2013), "*a meta-model means to a model what the model itself means to the real world. Loosely speaking, it is the model of the model*".

A computational (numerical) model - denoted here as $\mathcal{M}(\cdot)$ - is a deterministic black-box that describes the behaviour of a system ($\mathbf{y} \in \mathbb{R}^Q$) as a function of input variables ($\mathbf{x} \in \mathbb{R}^d$). It should be noted that since the input is a random vector, the output would also be random (Sudret, 2012). Taking this into account, meta-models - represented by $\hat{\mathcal{M}}(\cdot)$ - aim to mimic the response by approximating the computational model (Kroetz et al., 2017). Given the approximate nature of meta-models, their use increases the epistemic uncertainty of the assessed reliability (Dubourg et al., 2013; Sudret, 2012). It is worth noting that it seems possible to surrogate the violation probability as a function of the random vector; however, a reliability analysis must be performed for each point of the training dataset, which consequently requires significant recalls of the computational model. Therefore, in this study, the concept of meta-modelling is limited to approximating the response of the structure, which can be expressed as:

$$\mathbf{y} = \mathcal{M}(\mathbf{x}) \approx \hat{\mathcal{M}}(\mathbf{x}) \quad (3.1)$$

Referring to the reliability integral in Eq. 2.17, two general approaches can be followed to train meta-models, i.e., predicting the real value of the response (known as the *regression* problem) or distinguishing the situation as failure or safe (known as the *classification* problem). In other words, the latter surrogates the indicator function in the reliability integral. Various methods such as polynomial response surfaces, Gaussian process regression (Kriging), polynomial chaos expansion (PCE), support vector machines (SVM), k -nearest neighbour (k -NN), decision trees and artificial neural networks (ANN) have been used for this objective. It is worth noting that both of these general approaches are used in this study and a brief description of each adopted meta-model is presented in the coming sections. It

CHAPTER 3. META-MODELLING

should be emphasized here that the motivation of employing these approaches in this study is their assistance in significant reduction of computational time. The very expensive computational costs arise because of assessing reliability of desired bridges in a wide range of operating train speeds. Hence, not only many recalls of the computational model at each operating train speed is needed, but also the occurrence of resonance phenomenon at particular speeds increases the nonlinearity of the performance function.

The procedure of constructing meta-models is similar to that used for training machine learning models. Therefore, a supporting or *training dataset* is needed, which should be collected by designing experiments, and the model should then be validated to ensure its accuracy when dealing with unseen data. The former involves generating representative realizations of the input variables, feeding them into the computational model, and computing the desired responses. This results in obtaining a set of discrete estimates of the output as a function of the input vector (see Eq. 3.2).

$$\mathcal{S} = \{(\mathbf{x}^{(i)}, \mathbf{y}^{(i)}), \quad i = 1, 2, \dots, N\} \quad (3.2)$$

This procedure requires calling the original computational model. Therefore, it is obvious that the size of the training dataset should be kept as small as possible, otherwise the main goal of using meta-models would be violated. In this context, it is recommended to use stratified sampling techniques to generate a sample pool. Furthermore, the initial size of the training dataset should be of the order of $N = 10d$ as a rule of thumb, where d is the number of contributing random variables (Jones et al., 1998).

Then, the defining parameters of the meta-model can be computed using various techniques such as the least square method or maximum likelihood. It should be emphasized that the trained meta-models are susceptible to both *over-fitting* (high variance) and *under-fitting* (high bias) issues. Therefore, it is important to evaluate their performance for unseen situations. This can be achieved by selecting new realizations from the sample pool and revisiting the original model to create a test set; however, it is obvious that this approach increases the computational cost. Therefore, it is recommended to compute the cross-validation error, in particular the leave-one-out one (ϵ_{LOO}). This error is the special case of k -fold cross-validation, where one point is excluded from the dataset at each step and the model is trained with the remaining data. In other words, the number of foldings is equal to the size of the training dataset. Then, the error is estimated using the excluded data points. Finally, the error of the model is given as the mean of these errors (see Eq. 3.3).

$$\epsilon_{LOO} = \frac{1}{N} \sum_{i=1}^N \mathcal{L}[\mathbf{y}(\mathbf{x}^{(i)}), \hat{\mathbf{y}}_{-i}(\mathbf{x}^{(i)})] \quad (3.3)$$

where, \mathcal{L} is the considered loss function, $\mathbf{y}(\cdot)$ is the true response obtained from the computational model and $\hat{\mathbf{y}}_{-i}(\cdot)$ is the predicted response by the cross-validated meta-model which in its training process the i th data point is removed from the training dataset. It can be either the absolute residual, the square of the residuals, or the standardized residual (Jones et al., 1998; Myers et al., 2016). If the trained model does not meet the desired level of accuracy, the training dataset should be enriched with new sample point(s). Obviously, it is not necessary for the meta-model to be accurate in the subject of reliability evaluation on the whole problem space. On the contrary, it should be more accurate near the limit state function. This enrichment aspect is known as *adaptive sampling* and is discussed separately in the next section.

It is clear that as the size of the training dataset increases, the accuracy of the meta-model would probably increase, but on the other hand, the performance of the reliability integral evaluation would decrease. Therefore, a fundamental question arises, namely whether the chosen type of meta-model is suitable for the aimed problem or not. In this regard, an extensive literature review was conducted in Alizadeh et al. (2020), which led to general suggestions for the selection of meta-models considering the three factors of dataset size, accuracy and computation time for the evaluation of the trained model. A similar study was conducted in Kroetz et al. (2017) where the performance of ANN, PCE and Kriging meta-modelling is compared in different benchmark problems. It was found that despite good performance of all methods, the PCE method may suffer from the curse of dimensionality. Moreover, it is worth noting that the conventional polynomial response surface method loses its advantage in the case of considerably nonlinear limit states (Labeyrie, 1997; Sudret, 2012).

In summary, it is important to use meta-models cautiously because there is no guarantee that the violation probability (\hat{p}_f) evaluated with them is equal to the true failure probability (p_f). In other words, \hat{p}_f is not an unbiased estimate of p_f (Sudret, 2012). Considering this fact, several studies combined meta-modelling with other techniques, such as important sampling, to overcome this problem. Such approaches are not used in this study; hence, the interested reader is referred to Dubourg et al. (2013).

3.1 Adaptive enrichment

In this section, a brief overview of approaches that can be followed to add new sample point(s) to the initial one is presented. This procedure is called *adaptive sampling* or *sequential experimental design*. The general concept of these approaches is based on increasing our knowledge of regions about which we either have less information (large variance) or which have a large impact on our reliability assessment (close to the limit state). A comprehensive literature review on adaptive

CHAPTER 3. META-MODELLING

approaches can be found in Teixeira et al. (2021), to which the interested reader is referred, and to the references therein.

Based on Santner et al. (2003), the amount of information in an experiment is related to *entropy*. It is defined as expected value of the *surprise*; which in turn is defined as logarithm of the inverse probability. Therefore, the amount of information in the parameters of the trained model (θ) after the experimental design of \mathcal{S} reads as Eq. 3.4, which must be maximized by selecting new sample points. The other approach can be to minimize the standard mean squared prediction error (MSPE). It is obvious that using these approaches requires calling a computational model; therefore, as claimed in Santner et al. (2003), they are not so popular in practice.

$$I_{\mathcal{S}} = \int [\theta|\mathcal{S}] \ln [\theta|\mathcal{S}] d\theta \quad (3.4)$$

$$\text{MSPE}[\hat{\mathbf{y}}(\mathbf{x})] = \mathbb{E}[(\hat{\mathbf{y}}(\mathbf{x}) - \mathbf{y}(\mathbf{x}))^2] \quad (3.5)$$

$$\mathbf{x}^* = \underset{x}{\operatorname{argmin}} \int_{\mathcal{D}} \frac{\text{MSPE}[\hat{\mathbf{y}}(\mathbf{x})]}{\sigma^2} \omega(\mathbf{x}) d\mathbf{x} \quad (3.6)$$

where, \mathcal{D} is the feasible domain of the random variables, σ^2 is the standard deviation, and $\omega(\cdot)$ is the non-negative weight functions whose sum in the feasible domain equals one.

To overcome this issue, the well-known *Efficient Global Optimization* (EGO) is presented in Jones et al. (1998). In this approach, the most uncertain points of the trained model can be found by maximizing the *expected improvement* (see Eq. 3.7). The inherent advantage of this method is that the computational model does not need to be evaluated except for the new sample point. To facilitate solving the optimization problem, the authors in Jones et al. (1998) made a great effort to determine the boundaries of the problem; however, they are presented for the case of the Kriging meta-model. Note that the procedure terminates when the expected improvement falls below 1%.

$$EI(\mathbf{x}) = \mathbb{E}[\max(f_{\min} - \hat{\mathbf{y}}(\mathbf{x}), 0)] \quad (3.7)$$

where, f_{\min} is the minimum of the trained meta-model.

Based on Echard et al. (2011), the potential points to be considered in each iteration of adaptive sampling should satisfy at least one of these criteria, i.e., be close to the limit state function where a small error in the prediction will cause them to be misclassified as safe or failed and have a large uncertainty. In this context, a learning function denoted as *U-criterion* is proposed (see Eq. 3.8), which is simply a reliability index of $\text{sign}[\mathbf{y}(\mathbf{x})] \neq \text{sign}[\hat{\mathbf{y}}(\mathbf{x})]$. It should be noted that the criterion is proposed for the Kriging meta-model, where the standard deviation of each prediction can be easily calculated. Then, the best candidate for the next

3.1. ADAPTIVE ENRICHMENT

sample point can be determined among those in the sample pool with the smallest U -criterion value. Furthermore, it is believed that those points with U -criterion value greater than 2 do not have significant uncertainty to be added to the training dataset. It worth noting that the procedure stops when the coefficient of variation of the predicted violation probability using trained meta-model becomes less than the prescribed limit (e.g. 0.05). For the same approach, maximum difference between evaluated safety index by the trained meta-model and those estimated by 95% lower and upper confidence bounds is introduced in Dubourg et al. (2011) as the stopping criteria. It is proposed for the stopping limit to be about 0.1-0.01.

$$U(\mathbf{x}) = \frac{|0 - \hat{\mathbf{y}}(\mathbf{x})|}{\sigma_{\hat{\mathbf{y}}}} \quad (3.8)$$

Similar to the U -criterion, a "max-min" sampling scheme is presented in Basudhar and Missoum (2010), which assumes that the region with the largest distance to the existing dataset has the largest uncertainty. Moreover, considering a point that is close to the current approximated limit state has a larger impact on the change of the trained meta-model than those that are far from it. This approach leads to obtaining the new sample point by solving the optimization problem presented as:

$$\begin{aligned} \min_{\mathbf{x}, z} \quad & -z \\ \text{s.t.} \quad & \begin{cases} \|\mathbf{x} - \mathbf{x}_i\| \geq z & i = 1, 2, \dots, N \\ \hat{g}(\mathbf{x}) = 0 \end{cases} \end{aligned}$$

where, z is an arbitrary parameter defined to overcome non-differentiability of the cost function.

A later revision of this approach presents a generalized form that takes into account the joint probability between random variables. Then, the Chebychev distance was used to construct an unconstrained optimization problem as Eq. 3.9 (Lacaze and Missoum, 2014). It is worth mentioning that the stopping criteria in this approach is based on the relative change of the polynomial coefficients of the trained meta-model, which is originally considered as SVM.

$$\begin{aligned} \min_{\mathbf{x}} \quad & -\frac{1}{d} \log f_{\mathbf{X}}(\mathbf{x}) + \frac{1}{q} \log \sum_{i=1}^N \|\mathbf{x} - \mathbf{x}_i\|^{-q} \\ \text{s.t.} \quad & \mathbf{x} \in \Omega_F \end{aligned} \quad (3.9)$$

where, $f_{\mathbf{X}}(\mathbf{x})$ is the joint probability distribution of the basic random variables, q is a very big constant number such as 40 and Ω_F is the failure domain.

3.2 Ensemble models

The above aspects all referred to a single meta-model; however, it is possible to combine several individual (heterogeneous) models into a committee and predict the final outcome based on their decisions. The final prediction can be obtained by averaging in regression problems (see Eq. 3.10), by majority voting in classification problems (see Eq. 3.11), or by probabilistic methods in both. This approach is commonly known as *ensemble learning* (Goel et al., 2007; Sammut and Webb, 2011).

$$\hat{\mathcal{M}}(\mathbf{x}) = \sum_{j=1}^m \omega_j \hat{\mathcal{M}}_j(\mathbf{x}) \quad (3.10)$$

$$\hat{\mathcal{M}}(\mathbf{x}) = \text{sign} \left[\sum_{j=1}^m \omega_j \hat{\mathcal{M}}_j(\mathbf{x}) \right] \quad (3.11)$$

Note that the result of the classification model can be either +1 or -1 (i.e. categorical discrete data type representing failure or safety classes).

Regarding the combination of the individual meta-models, mostly identical constant weights are considered for all of them; however, three other different strategies are proposed in Goel et al. (2007) as:

$$\omega_j = \begin{cases} 1, & \epsilon_j = \min(\epsilon_{i=1,\dots,m}) \\ 0, & \text{Otherwise} \end{cases} \quad (3.12)$$

$$\omega_j = \frac{\sum_{i=1, i \neq j}^m \epsilon_i}{(m-1) \sum_{i=1}^m \epsilon_i} \quad (3.13)$$

$$\omega_j = \frac{(\epsilon_j + a\epsilon_{\text{ave}})^b}{\sum_{i=1}^m (\epsilon_i + a\epsilon_{\text{ave}})^b} \quad (3.14)$$

where, ϵ_i is the leave-one-out cross validation error of the i -th individual meta-model, m is the number of considered individual meta-models and ϵ_{ave} is the mean of leave-one-out cross validation errors. Furthermore, a and b are constant values which control the importance of average model compared to that of the individual models. They are proposed to be taken as 0.05 and -1, respectively.

It is necessary for the individual models to be diverse. In other words, they should not make identical mistakes or their errors should be uncorrelated. To this end, several methods have been developed, which the interested reader may refer to Sagi and Rokach (2018) and the references therein. Among them, *Bagging* (Bootstrap Aggregating) and *AdaBoost* are the most well-known methods. The former trains

each individual model using a dataset sampled from the original dataset with replacement. This means that some points are excluded and some others can be repeated within this dataset. In this case, the individual models would be independent. However, the latter trains dependent models by focusing on misclassified cases and increasing their weight in subsequent iterations, while decreasing the weight of correctly classified cases.

The discussed methods use the identical type of model within their procedure; however, it is possible to ensemble different model types to construct *stacked models*. A schematic view of the concept is shown in Figure 3.1. In general, the original dataset is used to train individual models in the first layer of the stacked model; however, their cross-validated predictions create a new dataset to train the model in the second layer (Sagi and Rokach, 2018).

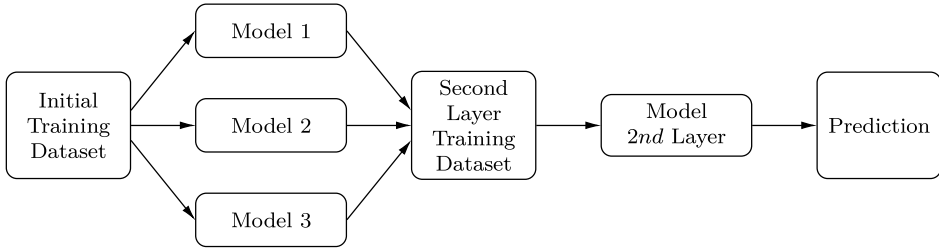


Figure 3.1: Schematic representation of the stacked models.

In summary, Cheng and Lu (2020) has applied ensemble learning of conventional meta-models, e.g., Kriging, PCE, and SVM in benchmark reliability assessment problems, where a very good estimate of violation probability is obtained with much smaller number of recalling computational models. In this study, each meta-model was adaptively trained using the U -criterion; while the stopping criteria was based on the relative difference between the maximum and minimum estimated violation probability from each of the models. Moreover, the weighting function of Eq. 3.14 was adopted to ensemble the individual meta-models. It should be emphasized that the required model evaluations of the method were even less than previously described adaptive methods.

3.3 Gaussian process (Kriging)

In general, the Gaussian process is a stochastic process that generalizes the concept of Normal distribution in the scale of random variables to function. Thus, it is a collection of random variables, each subset of which also has a common Gaussian distribution. Such models have very interesting properties that have led them to

CHAPTER 3. META-MODELLING

receive a lot of interest in machine learning and meta-modelling applications. For example, they can be completely defined in terms of their mean and covariance matrices. In this section, a brief overview of their concepts is presented. The interested reader can find more detailed information in Jones et al. (1998); Rasmussen and Williams (2006); Rogers and Girolami (2020) and the references therein. It should be noted here that the Gaussian process can be used for both regression and classification purposes; however, only the regression process is used in this study. Therefore, the description of its formulation for classification problems is omitted here.

As mentioned earlier, the objective of using meta-models is to predict unseen data given a dataset that contains true observed values corresponding to an arbitrary input (training dataset in Eq. 3.2). Assuming the model of $\hat{\mathcal{M}}(\cdot)$ with a vector of parameters as \mathbf{w} , since the parameters are defined based on a limited information, then they can be considered as a random variable. Considering the Bayesian approach, the posterior distribution of the model parameters given the training dataset would be as:

$$P(\mathbf{w}|\mathbf{X}, \mathbf{y}) = \frac{P(\mathbf{y}|\mathbf{w}, \mathbf{X})P(\mathbf{w})}{\int P(\mathbf{y}|\mathbf{w}, \mathbf{X})P(\mathbf{w})d\mathbf{w}} \quad (3.15)$$

where, $P(\mathbf{w})$ is the prior distribution of the parameters.

Then the new prediction for the unseen data of \mathbf{x}^* can be obtained using Eq. 3.16. Since the integration is computed over all values of the parameters, the Gaussian process is called a *non-parametric model*.

$$P(\mathbf{y}^*|\mathbf{x}^*, \mathbf{X}, \mathbf{y}) = \int P(\mathbf{y}^*|\mathbf{x}^*, \mathbf{w})P(\mathbf{w}|\mathbf{X}, \mathbf{y})d\mathbf{w} \quad (3.16)$$

Now the model in its simplest form can be assumed to be similar to the linear regression problem, leading that to be formulated as:

$$\hat{\mathcal{M}}(\mathbf{x}) = \mathbf{y} = \mathbf{g}(\mathbf{x}) + \epsilon(\mathbf{x}, \theta, \sigma^2) = \mathbf{f}(\mathbf{x})^\top \mathbf{w} + \epsilon(\mathbf{x}, \theta, \sigma_n^2) \quad (3.17)$$

where, $\mathbf{g}(\mathbf{x})$ is the noise-free prediction vector, $\mathbf{f}(\mathbf{x})$ is a matrix collecting the vector of predefined fixed basis functions of \mathbf{x} (usually taken as polynomials), \mathbf{w} are the unknown coefficients to be estimated and $\epsilon(\mathbf{x}, \theta, \sigma^2)$ is a stationary Gaussian process with zero mean and autocovariance function of $k(x, x')$ which reads as:

$$\epsilon(\mathbf{x}, \theta, \sigma^2) \sim \mathcal{GP}(0, k(\mathbf{x}, \mathbf{x}')) \quad (3.18)$$

Unlike linear regression, the Gaussian process does not consider the errors to be independent. On the contrary, it assumes that the confidence of the predictions is

3.3. GAUSSIAN PROCESS (KRIGING)

related to the distance of the new unseen point from the points whose true values are known. In other words, if the unseen point is close to a point whose we know its true value, we have more information about possible values of this point compared to the cases far from known points. The Gaussian process implements this using the autocovariance function (known as *kernel*). A variety of kernel functions are proposed, of which the squared exponential (Eq.3.19) is the most commonly used. To distinguish the parameters of the kernel function from the parameters of the model, the former (represented here by θ) are referred to as *hyper-parameter*.

$$k_{np}(\mathbf{x}_n, \mathbf{x}_p) = \exp \left(- \sum_{i=1}^N \left(\frac{x_{ni} - x_{pi}}{\theta_i} \right)^2 \right) + \sigma_{np}^2 \delta_{np} \quad (3.19)$$

where, δ_{np} is the Kronecker delta and σ^2 is the variance of the noise in observations.

Assuming a Normal prior distribution for the parameters ($\mathbf{w} \sim \mathcal{N}(\mathbf{b}, \mathbf{B})$), the model would be the sum of two normally distributed functions, leading the likelihood to also have Gaussian distribution. Then the posterior distribution of parameters would be *conjugate* of the prior distribution, meaning that the posterior distribution would also be Gaussian. Consequently, the distribution of the prediction for unseen data would be Gaussian given the training dataset and the input. Moreover, the model is the sum of two Gaussian functions, hence it would be a Gaussian process as:

$$\hat{\mathcal{M}}(\mathbf{x}) \sim \mathcal{GP}(\mathbf{f}(\mathbf{x})^\top \mathbf{b}, k(\mathbf{x}, \mathbf{x}') + \mathbf{f}(\mathbf{x})^\top \mathbf{B} \mathbf{f}(\mathbf{x})) \quad (3.20)$$

Similarly, the joint distribution between the predicted values on the training dataset and the unseen data would be the Normal distribution according to Eq. 3.21.

$$\begin{bmatrix} \hat{\mathcal{M}}(\mathbf{x}) \\ \hat{\mathcal{M}}(\mathbf{x}^*) \end{bmatrix} \sim \mathcal{N} \left(\begin{bmatrix} \mathbf{F}(\mathbf{x})^\top \mathbf{b} \\ \mathbf{F}(\mathbf{x}^*)^\top \mathbf{b} \end{bmatrix}, \begin{bmatrix} \mathbf{K}(\mathbf{X}, \mathbf{X}) + \sigma_n^2 \mathbf{I} & \mathbf{K}(\mathbf{X}, \mathbf{X}^*) \\ \mathbf{K}(\mathbf{X}^*, \mathbf{X}) & \mathbf{K}(\mathbf{X}^*, \mathbf{X}^*) \end{bmatrix} \right) \quad (3.21)$$

where, $K(\cdot, \cdot)$ and $F(\cdot)$ are the collective matrices of covariances and basis functions. The equations are simplified by considering $\mathbf{K}_{11} = \mathbf{K}(\mathbf{X}, \mathbf{X}) + \sigma_n^2 \mathbf{I}$, $\mathbf{K}_{12} = \mathbf{K}(\mathbf{X}, \mathbf{X}^*)$, $\mathbf{K}_{21} = \mathbf{K}(\mathbf{X}^*, \mathbf{X})$, $\mathbf{K}_{22} = \mathbf{K}(\mathbf{X}^*, \mathbf{X}^*)$, $\mathbf{F} = \mathbf{F}(\mathbf{x})$ and $\mathbf{F}^* = \mathbf{F}(\mathbf{x}^*)$.

Then the conditional probability distribution of the predicted values at unseen data given the training dataset and input, would be a Normal distribution with mean and variance as Eqs. 3.22 and 3.23, respectively.

$$\mu^* = \mathbf{F}^{*\top} \hat{\beta} + \mathbf{K}_{22}^\top \mathbf{K}_{11}^{-1} (\mathbf{y} - \mathbf{F}^\top \hat{\beta}) \quad (3.22)$$

$$\sigma^{*2} = \mathbf{K}_{22} - \mathbf{K}_{21} \mathbf{K}_{11}^{-1} \mathbf{K}_{12} + R^\top (\mathbf{F} \mathbf{K}_{11}^{-1} \mathbf{F}^\top)^{-1} R \quad (3.23)$$

$$\hat{\beta} = (\mathbf{B}^{-1} + \mathbf{F} \mathbf{K}_{11}^{-1} \mathbf{F}^\top)^{-1} (\mathbf{B}^{-1} \mathbf{b} + \mathbf{F} \mathbf{K}_{11}^{-1} \mathbf{y}) \approx (\mathbf{F} \mathbf{K}_{11}^{-1} \mathbf{F}^\top)^{-1} \mathbf{F} \mathbf{K}_{11}^{-1} \mathbf{y} \quad (3.24)$$

$$R = \mathbf{F}^* - \mathbf{F} \mathbf{K}_{11}^{-1} \mathbf{K}_{22} \quad (3.25)$$

These equations lead to a conditional distribution of the predicted response for unseen data. The best prediction from this distribution should minimize the expected loss. It has been shown that the mean and median values of the distribution minimize the squared and absolute losses, respectively. Since the Gaussian distribution is symmetric, the median and mean are equal.

One of the advantages of the Gaussian process is the variance of the conditional distribution. This value measures the epistemic uncertainty of the model. Therefore, it gives an indication of the points that can be selected in the adaptive enrichment procedure (Dubourg et al., 2011).

Example 3.1- Crude MC assisted by Kriging Meta-Model

In this example, the problem presented in Example 2.1 is again solved using meta-model assisted crude MC. For this objective, the kriging meta-model surrogates the performance function.

Two different training datasets (in size) are considered, and their leave-one-out cross-validated performance is shown in Figure 3.2. It is worth noting that these two datasets were generated with the improved Latin Hypercube sampling technique using different seeds. As can be seen, the trained model with a dataset size of 40 (i.e., 10 times the number of basic random variables) satisfies the desired leave-one-out cross-validation error, which is usually between 0.1-0.001. Moreover, it should be emphasized that the meta-models perform better within the range of trained values. Considering this, the model with a data set of 20 is not able to accurately predict negative values of the performance function (i.e. the failure domain).

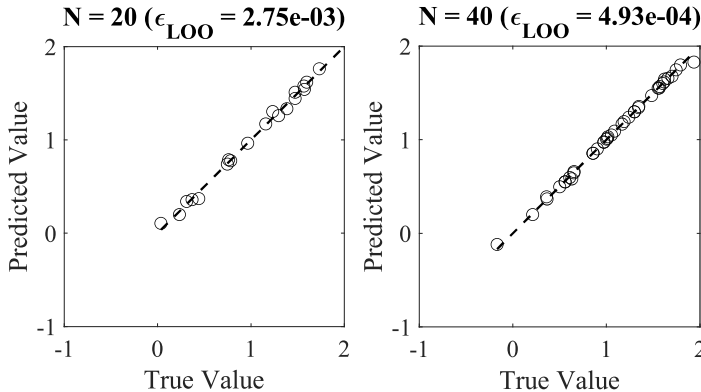


Figure 3.2: Performance of leave-one-out cross-validated Kriging meta-models with different training dataset sizes.

3.4. POLYNOMIAL CHAOS EXPANSION (PCE)

Next, the trained Kriging meta-model is used to conduct crude MC with a sample size of 10^5 ; where, the result of $\beta = 1.864$ is obtained. As can be seen, the computed safety index agrees acceptably with the benchmark solution.

It is worth noting that the computational cost of the metamodel-based MC is about 13.2% of the cost of the crude MC solution. The reported value excludes the time spent on training the meta-model. Clearly, the more complex the computational model, the greater the difference between these two approaches.

3.4 Polynomial chaos expansion (PCE)

The decomposition of complicated functions as a summation of simple orthogonal functions is a widely used concept in engineering problems, for example in the Fourier transform or modal analysis in structural dynamics. Polynomial chaos expansion (PCE) applies the same methodology; therefore, it can be a candidate to surrogate computational models with some basis functions. The concepts presented in this section are adapted from Blatman (2009); Blatman and Sudret (2011); Sudret (2008); Xiu and Karniadakis (2002). The interested reader can find more detailed information in these references and the references therein.

Two functions in Hilbert space are considered orthogonal if their inner product satisfies Eq. 3.26.

$$\langle \phi_n(x), \phi_m(x) \rangle_w = \int_{\mathcal{D}} \phi_n(x) \phi_m(x) w(x) dx = \gamma_n \delta_{nm} \rightarrow \phi_n(x) \perp \phi_m(x) \quad (3.26)$$

where, $w(x)$ is the density of measure function (also called *weighting function*), \mathcal{D} is its support, γ_n is the normalization constant, and δ_{nm} is the Kronecker delta.

Considering the orthogonality condition, for certain probability functions, a system of orthogonal polynomials can be found whose PDF is the same as the weighting function. These polynomials satisfy a *three-term recursion relation* as Eq. 3.27 and are the basis functions used in PCE.

$$A_n \phi_{n+1}(x) = (A_n + B_n - x) \phi_n(x) - B_n \phi_{n-1}(x) \quad n \geq 1 \quad (3.27)$$

where, A_n and B_n are nonzero constants, $\phi_{-1}(x) = 0$ and $\phi_0(x) = 1$.

PCE was originally developed for independent random variables with Gaussian distribution as weighting function. Obviously, the transformation concepts described in Section 2.1 can be applied to use the method for non-Gaussian random variables;

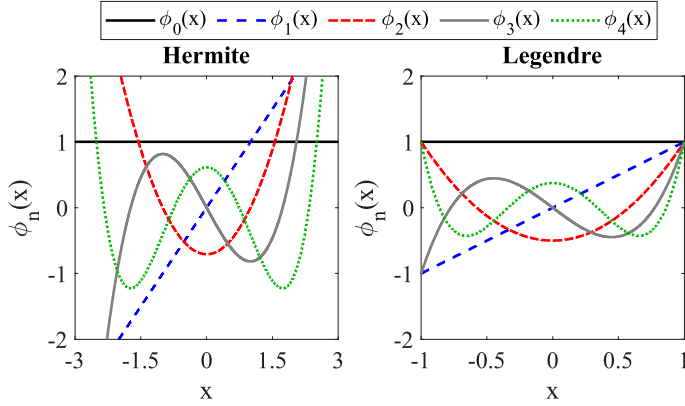


Figure 3.3: Hermit and Legendre polynomial chaos functions.

however, this method was later extended for other common probability distributions. The former is referred to as *Wiener polynomial chaos* and the latter as *Wiener-Askey polynomial chaos*. Some of the most commonly used ones are listed in Table 3.1. The first five curves of Hermite and Legendre polynomials are shown in Figure 3.3.

Table 3.1: Widely used Wiener-Askey polynomial chaos

Distribution	Wiener-Askey polynomial chaos	Support
Gaussian	Hermite	$(-\infty, \infty)$
Uniform	Legendre	$[-1, 1]$
Beta	Jacobi	$[-1, 1]$
Gamma	Laguerre	$[0, \infty)$

It has been shown that any function in the L_2 sense (finite variance, which is the case in practical situations) can be expanded as summation of tensor product of corresponding Wiener-Askey polynomial chaos functions. Therefore, the random process (here the computational model of $\mathcal{M}(\cdot)$) can be decomposed as:

$$\mathcal{M}(\mathbf{X}) = \sum_{\alpha \in \mathbb{N}^d} \mathbf{c}_\alpha \Psi_\alpha(\xi) \quad (3.28)$$

where, \mathbf{c}_α is the set of coefficients to be determined, $\Psi_\alpha(\xi)$ is the tensor product of the basis polynomial chaos functions, ξ is the vector of reduced form of the basic random variables and d is the dimensionality (number of basic random variables) of the original function. It is worthwhile noting that the Kronecker tensor product

3.4. POLYNOMIAL CHAOS EXPANSION (PCE)

of two vectors reads as:

$$\phi \otimes \phi' = [\phi_1 \quad \dots \quad \phi_n]^\top \otimes [\phi'_1 \quad \dots \quad \phi'_m]^\top = \begin{bmatrix} \phi_1 \phi'_1 & \phi_1 \phi'_2 & \dots & \phi_1 \phi'_m \\ \phi_2 \phi'_1 & \phi_2 \phi'_2 & \dots & \phi_2 \phi'_m \\ \vdots & \vdots & \ddots & \vdots \\ \phi_n \phi'_1 & \phi_n \phi'_2 & \dots & \phi_n \phi'_m \end{bmatrix} \quad (3.29)$$

The number of elements of the tensor product of two polynomial chaos functions with order of 5 is schematically illustrated as crosses and circles in Figure 3.4. It should be emphasized here that the idea of this figure is adapted from Blatman (2009).

It is obvious that the computational cost of summing infinite terms is not affordable; therefore, the highest order of the polynomials is needed to be truncated to q (see Eq. 3.30). Then, the cardinality of total degree (number of expansion terms) would be a function of the dimensionality and the highest order of the polynomials; which can be estimated by Eq. 3.31. In this case, the elements which should be implemented in the illustrative 2D example would decrease to circles only (see Figure 3.4).

$$\mathcal{M}(\mathbf{X}) \approx \hat{\mathcal{M}}(\mathbf{X}) = \sum_{|\alpha| \leq q} \mathbf{c}_\alpha \Psi_\alpha(\xi) \quad (3.30)$$

$$P = \frac{(d+q)!}{d!q!} \quad (3.31)$$

A further truncation scheme is presented by Blatman (2009) named as *hyperbolic index set*. In this approach a hyperbola is defined and all terms outside of this hyperbola would be truncated. The total degree in this approach reads as:

$$|\alpha|_\gamma = \left(\sum_{i=1}^d \alpha_i^\gamma \right)^{1/\gamma} \quad 0 < \gamma \leq 1 \quad (3.32)$$

Three different truncation scenarios using this approach is shown in Figure 3.4.

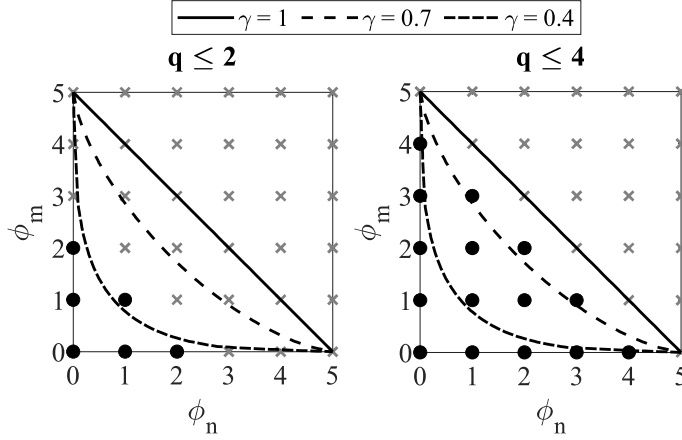


Figure 3.4: Total number of the expansion terms in PCE.

It is obvious that increasing the polynomial order can improve the accuracy of the PCE-based meta-model; however, it should be noted that this increases the computational cost of computing the constants. Consequently, calculating more constants requires a larger dataset (more recalls of the computational model). Therefore, training PCE would be a trade-off between accuracy and computational cost in the training phase.

Different methods are proposed to compute the coefficients of the polynomials, such as projection and least square minimization. The former uses the property of orthogonality to remove all coefficients except the one corresponding to the desired polynomial; this follows from Eq. 3.33. The left-hand side of this equation must be estimated using numerical integration methods; therefore, this may increase the computational cost of training.

$$\mathbb{E}[\Psi_\beta \mathcal{M}(\mathbf{X})] \approx \mathbb{E}\left[\sum_{|\alpha| \leq q} \mathbf{c}_\alpha \Psi_\beta(\mathbf{X}) \Psi_\alpha(\mathbf{X})\right] = \sum_{|\alpha| \leq q} \mathbf{c}_\alpha \mathbb{E}[\Psi_\beta(\mathbf{X}) \Psi_\alpha(\mathbf{X})] = \mathbf{c}_\alpha \quad (3.33)$$

On the other hand, the regression method finds coefficients by minimizing the sum of the residual squares. By collecting the true observed values from the computational model in the vector of \mathbf{f} and the corresponding values of the polynomials in the matrix of \mathbf{F} , the matrix of coefficients (\mathbf{C}) reads as:

$$\mathbf{C} = (\mathbf{F}^\top \mathbf{F})^{-1} \mathbf{F}^\top \mathbf{f} \quad (3.34)$$

3.5. SUPPORT VECTOR MACHINES (SVM)

Example 3.2- Crude MC assisted by PCE Meta-Model

In this example, the problem presented in Example 2.1 is again solved using the meta-model assisted crude MC. For this objective, the PCE meta-model surrogates the performance function. It should be emphasised here that these analyses were performed using the toolbox *UQLab* (Marelli and Sudret, 2014).

Due to the simplicity of the problem, the highest order of the polynomials is restricted to one or two. The performance of these two cases is compared in Figure 3.5. As can be seen, the second-order polynomials satisfy the desired leave-one-out cross-validation error of 0.001; thus, it acceptably resembles the performance function.

Then, using the trained meta-model, a crude MC with a sample size of 10^5 is performed. The result is $\beta = 2.086$, which is 11.4% higher than the benchmark solution. Moreover, it should be highlighted that the computational cost of the meta-model assisted crude MC was almost 0.5% of the crude MC.

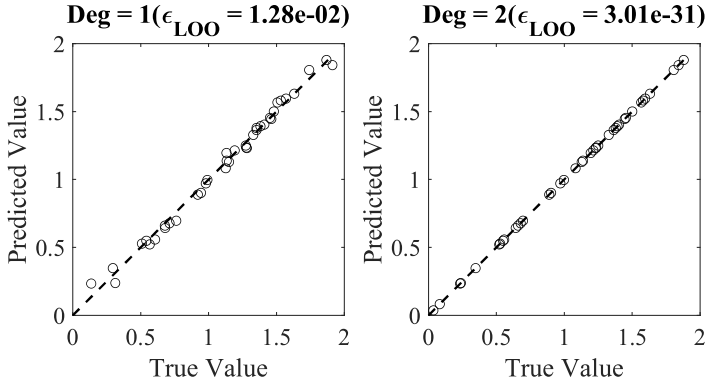


Figure 3.5: Trained PCE model.

3.5 Support vector machines (SVM)

The meta-models discussed so far attempt to approximate the computational model. However, considering the formulation of the simulation-based methods (Eq. 2.17), it would be possible to surrogate the indicator function instead. This is a binary function, which results in the meta-model problem switching from regression to classification. In this study, the Support Vector Machine (SVM), k -Nearest Neighbours (k -NN) and Decision Trees are used for this objective; therefore, an overview of their principles are presented in forthcoming sections. The concepts presented here for SVM are mainly adapted from Hurtado (2013), where the interested reader

CHAPTER 3. META-MODELLING

is referred to that and the references therein.

The main objective of SVM is to find a hyperplane (e.g., Eq. 3.35 in linearly separable cases) that separates different classes (in structural reliability, the safe and the failure domains). In binary problems, the prediction is made based on the sign of the resulting value from the hyper-plane definition (Eq. 3.36).

$$f(\mathbf{X}) = \langle \mathbf{w}, \mathbf{X} \rangle + b = 0 \quad (3.35)$$

$$\hat{\mathcal{M}}(\mathbf{x}^*) = \text{class}(\mathbf{x}^*) = \begin{cases} +1, & \text{sign}[f(\mathbf{x}^*)] > 0 \\ -1, & \text{sign}[f(\mathbf{x}^*)] < 0 \end{cases} \quad (3.36)$$

where, $\langle \cdot, \cdot \rangle$ is the inner product of two vectors, \mathbf{w} represents the normal vector of the hyper-plane and $f(\mathbf{x}^*)$ is called *classification score*.

Obviously, there are many choices of hyperplanes. Therefore, the goal is to find the best candidate, which is introduced as the one with the maximum distance to the nearest points. Moreover, it should have an identical distance to the nearest point in each class. It is worth noting that these points are known as *support vectors* and the absolute value of their predicted response is equal to one. This premise basically means that the method assigns unseen data in the range of two classes the same chance of belonging to one of the two classes. Since the distance of any point to a plane is inversely proportional to the norm of the normal vector, the problem would change to minimizing $1/2 \mathbf{w}^\top \mathbf{w}$ ($1/2$ comes from the width of the region between two classes - *margin*). In addition, the optimization problem is subjected to the constraints imposed by Eq. 3.36 and the definition of the support vectors; which is Eq. 3.37.

$$f(\mathbf{x}^*)[\langle \mathbf{w}, \mathbf{x}^* \rangle + b] \geq 1 \quad (3.37)$$

Then training the SVM would be solving a quadratic optimization problem, which in Lagrangian form reads as Eq. 3.38. As can be seen, solving this equation reduces the problem to minimising only Lagrange multipliers.

$$\begin{aligned} \mathcal{L} = \frac{1}{2} \|\mathbf{w}\|^2 - \sum_{i=1}^N \alpha_i \left[f(x_i)(\langle \mathbf{w}, \mathbf{x}_i \rangle + b) - 1 \right] = \\ \sum_{i=1}^N \alpha_i - \frac{1}{2} \sum_{i=1}^N \sum_{j=1}^N \alpha_i f(x_i) \langle \mathbf{x}_i, \mathbf{x}_j \rangle \alpha_j f(x_j) \end{aligned} \quad (3.38)$$

where, $\alpha_i \geq 0$ is the Lagrange multiplier.

The above formulation was developed for linearly separable classes; however, it is evident from Eq. 3.38 that the problem is only related to the inner product of the input points. As discussed earlier for Gaussian process regression, it is possible to

3.5. SUPPORT VECTOR MACHINES (SVM)

implicitly handle this situation using kernel functions. In summary, an example of SVM performance in a 2D nonlinear problem is depicted in Figure 3.6.

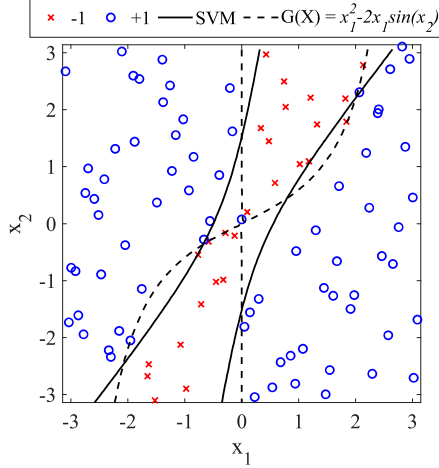


Figure 3.6: Example of SVM performance for a nonlinear limit state.

Example 3.3- Crude MC assisted by SVM Meta-Model

In this example, the problem presented in Example 2.1 is again solved using the meta-model assisted crude MC. For this objective, the SVM meta-model surrogates the performance function.

Three features, namely the speed parameter (S), the load to the flexural rigidity ratio (denoted here as F - each parameter in this ratio is normalized by its mean value), and the normalized vertical acceleration limit are considered for training the SVM meta-model. Moreover, a simple linear kernel function is employed due to apparent distinct safe and failure domains.

Similar to the previous examples, the leave-one-out cross-validation error is limited to a maximum of 0.001. To achieve this accuracy, the adaptive sample enrichment method proposed in (Lacaze and Missoum, 2014) (see Eq. 3.9) is applied. The performance of the trained model along with the initial training dataset and the adaptively added samples is shown in Figure 3.7.

Next, crude MC with a sample size of 10^5 is performed using the trained SVM-based meta-model, resulting in $\beta = 1.977$. Comparing this result with the benchmark solution, there is a difference of about 5.6%. It should be emphasized that the computational cost of running these simulations is about 0.3% of the crude MC using the original computational model. It

should be emphasized that the training time is not included in the reported cost of the meta-model assisted crude MC.

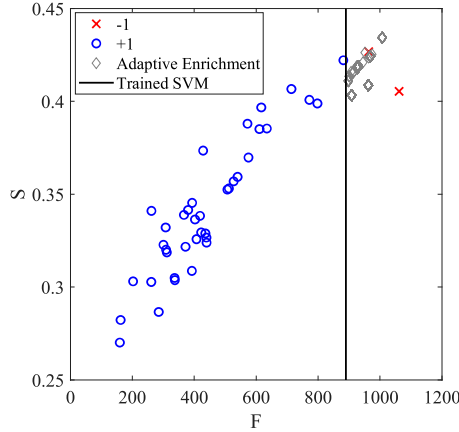


Figure 3.7: Trained SVM model.

3.6 K-Nearest Neighbours (k-NN)

K -NN is a classification algorithm similar to the SVM; which simply classifies the unseen data based on its distance to the k nearest neighbours. After distinguishing the neighbours, the class of their majority is assigned to the unseen data. A brief overview of this algorithm is presented here and the interested reader is referred to Rogers and Girolami (2020) for detailed information.

It is obvious that the performance of the algorithm depends on the selected number of neighbours. The small numbers makes the predictions to be highly influenced by noises and the large values may prevent the method to recognize the true patterns. Therefore, it is recommended for the best number of neighbours to be chosen by calculating the cross-validation error for a range of different k values. It should be noted that in the binary classification problems (such as reliability assessment problems), the model using even k value may fail to predict when the number of each class at neighbours become equal. This issue can be solved by considering an odd value for k or weighting neighbours based on their distance to the new data.

Example 3.4- Crude MC assisted by k -NN Meta-Model

In this example, the problem presented in Example 2.1 is again solved using the meta-model assisted crude MC. For this objective, the k -NN meta-model surrogates the performance function.

The number of neighbours is varied between 1-20 and the best k value is selected based on calculated leave-one-out cross validation error at each iteration (see Figure 3.8). As can be seen, $k = 2$ & 4 result in the smallest leave-one-out cross validation error; which the larger value is selected for further analyses.

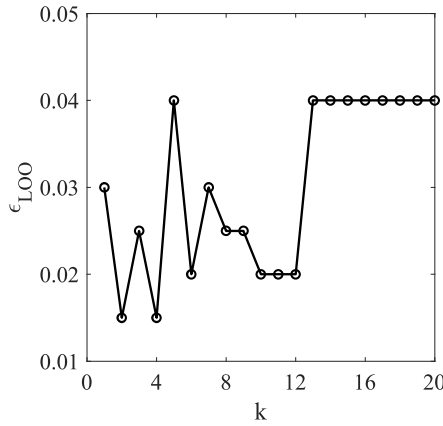


Figure 3.8: Performance of the k -NN meta-model as a function of considered neighbours.

Next, crude MC with a sample size of 10^5 is performed using the trained k -NN meta-model, resulting in $\beta = 2.064$. Comparing this result with the benchmark solution, there is a difference of about 10.6%. It should be emphasized that the computational cost of running these simulations is about 1.03% of the crude MC using the original computational model which shows a significant reduction.

3.7 Decision Tree

Decision trees are one of the widely used classification algorithms that can be easily interpreted. It is worthwhile noting that they can be employed for regression objectives also; however, this aspect is not used in this study. They are basically a flowchart (set of yes/no questions) starting from the root (the initial node), subdividing (breaking) the complex space of the problem through branches with simple choices at each step and predicting the class of data at leaves.

This is a "top-down" procedure which progresses by selecting the best splitting feature at each step of training. This feature is selected by calculating the weighted *impurity* or *entropy* of all features at the remaining sub-space of that step. These methods are called *Gini Index* (see Eq. 3.39) and *Info Gain* (see Eq. 3.40), respectively.

$$GI = \sum_k w^{(k)} \left[1 - \sum_j p_j^2 \right] \quad (3.39)$$

$$IN = \sum_k w^{(k)} \left[- \sum_j p_j \log(p_j) \right] \quad (3.40)$$

where, k is the number of sub-spaces at each step, j is the number of classes, $w^{(k)}$ is the weight of each sub-space (i.e. ratio of the data in that sub-space to the total number of data in that step) and p_j is the probability of a sample belonging to each class at each sub-space.

This procedure may result in a very deep decision tree which will probably be prone to the over-fitting issue. Therefore, a subtree of that is selected afterwards for further predictions; which results in smaller cross-validation error than the initial model. This procedure is known as *pruning*; which the interested can find detailed information about that in James et al. (2013).

It should be highlighted here that the single decision tree models mostly present a weak performance on complex problems. Therefore, several approaches such as *bagging*, *boosting* and *random forest* have been developed; which are basically a weighted combination of many decision trees.

Example 3.5- Crude MC assisted by Decision Tree Meta-Model

In this example, the problem presented in Example 2.1 is again solved using the meta-model assisted crude MC. For this objective, the decision tree meta-model surrogates the performance function.

Initially, the best maximum number of splits (branches) is obtained by calculating leave-one-out cross validation error for different considered values in the range of 1-10 (see Figure 3.9). As can be seen, the maximum 4 number of splits results in the model with the least error. This configuration is used to train the meta-model; which is presented in Figure 3.10.

Next, crude MC with a sample size of 10^5 is performed using the trained meta-model, resulting in $\beta = 1.953$. Comparing this result with the benchmark solution, there is a difference of about 4.7%. It should be emphasized that the computational cost of running these simulations (excluding the time spent on training the meta-model) is about 0.4% of the crude MC using the original computational model.

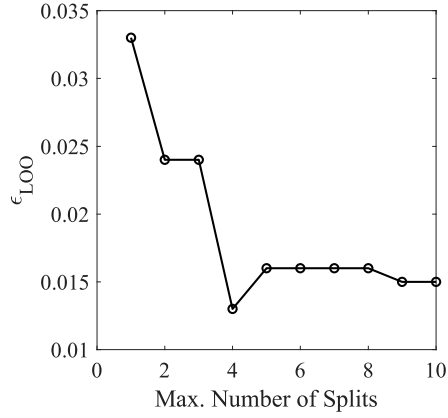


Figure 3.9: Performance of the decision tree meta-model as a function of maximum number of splits.

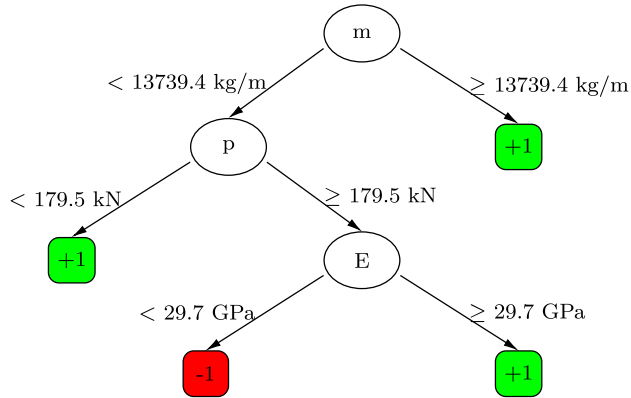


Figure 3.10: Trained decision tree meta-model.

Chapter 4

Summary of appended papers

High-speed railway transportation systems are becoming increasingly common around the world and are a more sustainable and reasonably time-efficient choice than airborne or road-based options for short- and medium-distance travels. The operation of trains with higher speed and/or axle load compared to traditional trains, brings new challenges, both for the existing infrastructure and for those to be built. It is evident that modern high-speed trains induce larger vibration levels on bridges, which they are not fully addressed in previous editions of design guidelines. In this regard, many studies have been carried out in the last two decades investigating different aspects of this problem. Nevertheless, most of them solved the problems of interest using deterministic approaches. This led to the fact that the current design or evaluation rules are subjective and various vague aspects can be distinguished. The latter statement is also addressed in previous studies. Therefore, this study is devoted to the application of probabilistic approaches to investigate some of these vague design methods of high-speed railway bridges. The application of different reliability assessment methods in the context of dynamic problems is evaluated and some preliminary conclusions are derived to provide a possible roadmap for future research. A brief overview of the appended papers are presented in this section. For general overview, the work flow and qualitative relation between papers are presented in Figure 4.1.

Paper I: Reliability assessment of the dynamic behavior of high-speed railway bridges using first order reliability method

Running safety, and in particular ballast destabilization, is shown to be a dominant design criterion for high-speed railway bridges. Previous experimental studies have shown the direct relationship between the vertical acceleration of the deck and this limit state (Zacher and Baessler, 2005). Therefore, design guidelines limit the vertical acceleration of the bridge subjected to the passage of trains at targeted operating speeds. To this end, a safety factor of 2 is assigned to the reported threshold value from experimental studies, which results in limiting the vertical deck acceleration of ballasted railway bridges to 3.5 m/s^2 .

To the authors' knowledge, there is no scientific background other than engineering judgement behind the selection of the above safety factor. Therefore, there is a possibility of designing either unnecessarily heavy or unsafe bridges. In order to identify such inconsistencies, a preliminary reliability-based evaluation is conducted

CHAPTER 4. SUMMARY OF APPENDED PAPERS

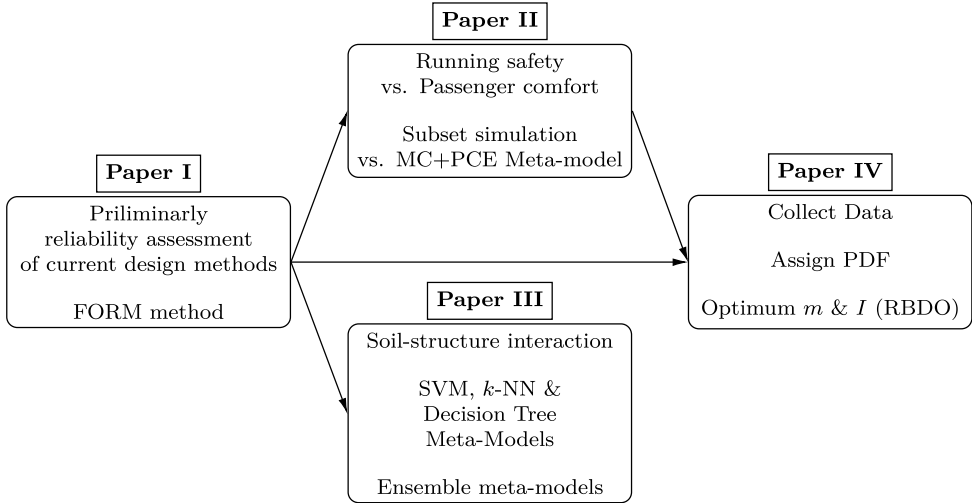


Figure 4.1: Work flow of the appended papers.

in Paper I. The objective was to obtain the design speed of generic bridges with similar characteristics to the existing ones, using both conventional deterministic approaches and probabilistic methods. It is necessary to evaluate the reliability of the system (probability of failure) for each operating speed in a wide range. This range is considered to be [200-400] km/h. In order to derive some general conclusions, the span length of the considered bridges is assumed to be in the range of [5-30]m, which covers short to medium spans. It is worth mentioning that in this study, 2D Euler-Bernoulli beams were considered to model the dynamic response of bridges and the boundary conditions were assumed to be simply supported. Moreover, rail irregularities and train-track-bridge interactions were neglected. Considering this, the FORM was selected for the objective of this paper. Otherwise, an expensive computational cost should be accepted if simulation-based methods were chosen for reliability assessment. The author was aware of the possibility that accuracy might be compromised due to the limitations of FORM for problems of a similar nature to Paper I; nevertheless, this method appears to be acceptable for the objective of comparison.

At the Paper I stage, a limited information was available to the author on the properties of bridges. Therefore, it was decided to assign very simple distributions compatible with the case of limited knowledge. Therefore, mean, lower and upper bounds of the values were determined and probability distributions were assigned based on them. Obviously, some random variables were correlated. This aspect was neglected in this study; however, they were all tied to the bridge span length.

The author has a sense that this may compensate for simplification in terms of dependence.

Deterministic assessments were then performed using means and averages plus/minus one standard deviation of the basic random variables. The first speed at which the maximum vertical acceleration of the deck surpasses 3.5 m/s^2 was assumed to be the deterministic design speed. The probabilistic design speed was determined by calculating the average failure probability for each operating speed and then finding the first one at which the violation probability exceeds the target value of 10^{-3} . Also, the deterministic design speeds were used to find the corresponding safety index. This is an approximate method, but it can give an idea of what safety would be expected if the bridge were subjected to the passage of a train at deterministic design speed.

For the reasons stated above, the absolute values of the safety indices were not an important conclusion of this work. The main point was the observation of a considerable difference between the deterministic design speeds and the corresponding probabilistic speeds. A similar pattern was observed for the corresponding safety indices. Furthermore, it was found that despite the use of a constant safety factor in the conventional design methodology, it cannot be guaranteed that the final design will meet the desired safety level.

As a side conclusion, a sensitivity analysis was performed for basic random variables using direction cosine in the FORM. It was found that the coach length, the flexural rigidity, the geometry of the bridge (or its mass per length) and the damping of the system are the most important variables (Allahvirdizadeh et al., 2020).

Paper II: Surrogate-assisted versus subset simulation-based stochastic comparison between running safety and passenger comfort design criteria of high-speed railway bridges

In order to propose reliable and consistent design methods for future applications, it is important to investigate the relationship between established limit states with others. In other words, modifying a method without considering its impact on the overall performance of the system may cause other limit states to become dominant. In this context, a stochastic comparison is made between the running safety criteria (discussed in Paper I) and passenger comfort.

Passenger comfort refers to the acceleration experienced by the passenger, which is implicitly related to the deflection of the bridge. In this study, a moving load problem on simply-supported bridges is solved to model their dynamic behaviour. In addition to Paper I, an equivalent additional damping method and a stochastic amplification factor were used to account for the effects of train-track-bridge interaction and rail irregularities, respectively. Bridge span lengths are limited to 10 m,

CHAPTER 4. SUMMARY OF APPENDED PAPERS

20 m and 30 m. In addition, dynamic analyses were performed for operating train speeds in the range of [200-300] km/h.

The assigned probability distributions were taken from Paper IV, where statistical methods are applied to a more extensive database. Therefore, the dependencies between random variables, in particular mass per length and moment of inertia, were modelled using Copula functions. Then, simulation-based methods were used to compare these two limit states. For similar reasons as explained in Paper I, the crude Monte-Carlo simulation method was not applicable. Therefore, two different approaches, namely subset simulation and meta-model based crude MC were considered. It should be noted that the polynomial chaos expansion (PCE) method was chosen to surrogate the computational model.

First, the sensitivity of the subset simulation with respect to the sample size (N_s) and the conditional probability at intermediate events (p_0) was investigated in order to select the best configuration of the parameters. For this objective, the values (1000, 2000, 3000, 4000, 5000) and (0.05, 0.1, 0.2) were considered for N_s and p_0 , respectively. It was observed that $N_s = 4000$ and $p_0 = 0.1$ give acceptably accurate results. Similarly, the best performing meta-models were obtained by considering different polynomial degrees up to the maximum value of 10 and the hyperbolic truncation scheme in the range of [0.5-1.0]. The best meta-model should have a lower polynomial degree while its leave-one-out cross-validation error does not exceed 0.001.

Then, a crude MC with a sample size of 10^6 was performed for both performance functions on bridges with a span length of 20 m and an operating train speed of 240 km/h. The resulting safety index and elapsed time were used as a benchmark solution to compare the performance of the subset simulation and the surrogate-based MC. Both approaches were found to result in safety indices very similar to those reported by crude MC, while the computational cost was only about 2% of that. Both methods worked well, but the subset simulation was chosen for further investigation.

Using the subset simulation, the variation of the safety index as a function of the operating train speed was calculated for both performance functions. Based on the obtained results, the running safety limit state dominates over the passenger comfort; however, their difference becomes smaller for longer bridges and slower trains (Allahvirdizadeh et al., 2021b).

Paper III: Ensemble meta-models for running safety assessment of high-speed railway bridges considering soil-structure interaction effects

Papers I and II neglected the effects of soil-structure interaction (SSI) in the construction of computational models. SSI effects shorten the frequency of the system,

which consequently reduces the critical speed at resonance. On the contrary, they can increase the damping of the structure, which reduces the amplitude of the vibrations experienced. Considering these two contradictory conditions, it would be essential to evaluate violation probability of the running safety considering the effects of SSI. For this objective, a similar moving load problem was solved as in Paper II, substituting the boundary conditions with lumped springs and dashpots. It was previously shown that the properties of these springs and dashpots are a function of the soil properties, the depth of the stratum, the dimensions of the foundation and, most importantly, the bridge-soil frequency ratio.

The properties of the basic random variables were adapted from Paper IV. Due to the considerable uncertainty of the soil properties, it was decided to consider different groups of deterministic values that can resemble the real conditions. Therefore, the shear wave velocity, the depth of the stratum and the width-to-length ratio of the foundations were considered as (150, 300, 600) m/s, (0.5, 5.0, 10.0) m and (0.5, 1.0), respectively. It should be noted that bridge span lengths and operational train speeds varied in the range of [10-30] m and [200-300] km/h, respectively.

In this paper, classification-based meta-models (such as support vector machines, k -nearest neighbours and decision trees) were used as surrogates for the computational models. To improve the performance of the meta-models, the concept of stack modelling was used. The input to the second layer of the model is the weighted posterior probability of the weak models in the first layer. It is worth noting that the accuracy of the model was considered acceptable if the cross-validated misclassification error of it was less than 0.01. This approach led to the training of a single meta-model for the entire range of operational train speeds. Subsequently, the performance of one meta-model was compared with the corresponding results of crude MC, and acceptable agreement was observed.

Then, the trained models were employed to conduct crude MC reliability analyses in the above mentioned range of operating train speeds. Next, the maximum and minimum of the obtained results from semi-probabilistic approach of each bridge length is reported as the possible boundary of safety. Comparing the obtained results in Paper II with those obtained in this study, revealed that neglecting SSI effects in short span bridges may lead to an underestimated evaluation of the safety index for running safety. However, it would be possible to have an overestimated safety index by increasing the span length (Allahvirdizadeh et al., 2022).

Paper IV: Minimum design requirements of high-speed railway bridges using reliability-based optimization

In the papers previously discussed, probabilistic approaches were used to investigate various aspects of running safety on high-speed railway bridges. It was found that conventional design methods need to be modified. One approach that is probably

CHAPTER 4. SUMMARY OF APPENDED PAPERS

most relevant is to update the safety factor of the method. At the time of writing Paper IV the author was not sure whether the current vertical acceleration limit was accurate or not. There is very limited knowledge on this subject. Then, a different approach was taken by using the reliability-based design optimization (RBDO) method to keep the vertical acceleration limit value as it is, neglecting the traditional safety factor from the design methodology and proposing minimum bridge design values for mass per length and moment of inertia (stiffness) instead.

In the first stage an extensive review of data available in the literature on various aspects of the problem (bridge geometry, material properties, train properties, and ballast destabilization) was conducted. In this context, 458 bridges in the Swedish railway network were surveyed to extract their geometrical properties. This information did not necessarily correspond to high-speed lines; however, it gives an idea of the possible range of values. Regarding the axle load of the trains, information from 49 conventional high-speed trains operating at European Union was considered. In addition, information on the bogie, suspension and coaches of 62 high-speed trains from around the world was extracted to perform modal analysis to obtain a dataset of high-speed train dynamic characteristics (including fundamental frequency, modal mass and damping ratio). As mentioned earlier, only one study was specifically devoted to investigate the problem of ballast instability using experimental programs, but results of two other shaking table tests were found from which the relationship between acceleration and lateral motion of ballast particles can be derived.

Statistical approaches were then followed to assign the best theoretical probability distribution function for each basic random variable. The procedure included considering the nature of the variable (e.g., is it always positive or not), calculating higher moments, performing statistical tests with 5% significance level, plotting quantile-quantile graphs and calculating goodness of fit using mean square error. This approach led to the selection of the best theoretical distribution, or in other words the least bad distribution. Then, its parameters were calculated using the maximum likelihood method. It is worth noting that in the case of the vertical acceleration limit, a Gaussian distribution is assigned without following the above approaches and only due to the central limit theorem. This assignment is due to the fact that it seems to be a function of many parameters. Then, the parameters of the distribution are obtained from the mean and standard deviation of the extracted data. Gathering a reliable amount of information allowed the calculation of parameters of the Copula functions for those basic random variables that were assumed to be dependent, in particular mass per length and moment of inertia. First, the best type of Copula function was selected by calculating the Akaike information criterion (AIC) and the Bayesian information criterion (BIC). Then, their parameters were calculated by the maximum likelihood method.

In this study, a non-intrusive nested reliability-based design optimization was per-

formed. Gaussian process regression (Kriging) was selected for the meta-models due to its robust performance and their performance were adaptively enriched using U-criterion. The accuracy of the trained surrogate models were assured by controlling the coefficient of variation of the estimated violation probability by them, calculating the generalized safety indices and also limiting their leave-one-out cross-validation error to 0.01. Then, minimum allowable mass per length and moment of inertia was obtained for bridges with different span lengths. Similarly, these values were used to propose maximum allowable fundamental frequency of single span simply-supported high-speed railway bridges. In order to use these values in further applications, an exponential equation is fitted to minimum mass per length and maximum fundamental frequency (Allahvirdizadeh et al., 2021a).

Chapter 5

Concluding remarks

5.1 Discussion

Running safety is a specific terminology in the design of high-speed railway bridges. It refers to the prevention of derailments or any phenomena which endangers safe passage of trains over the bridge. Safety does not mean that failure will not occur in a component or system during its service life. Rather, it means that the probability of failure will not exceed a desired value during a specified period of time. This limit value depends on a large number of parameters, in which the consequences of a failure (risks) play a role above all. The latter can be categorized as fatalities/injuries, monetary, social and legal consequences of failure. Therefore, any study that aims to update the design rules in terms of running safety should first evaluate the probability of violating limit states and then calculate the consequences of exceeding these thresholds. It is obvious that this requires the consideration of the associated uncertainties in the problem. In other words, probabilistic approaches should be used.

This licentiate thesis aims to provide the basis for updating the current design regulations of high-speed railway bridges, especially with respect to their running safety. The ultimate goal is to propose new design methods that lead to both optimal and safe solutions. At this stage of the project, the consequences of failure are neglected. Then, the author has tried to understand the nature of the problem, collect information on its various aspects to assign appropriate probability distribution functions, evaluate the performance of various reliability assessment methods in this subject, study the effects of different parameters on the calculated failure probability or different limit states on the final design, and use reliability-based design optimization to propose minimum design requirements. Following this path resulted in papers with chronological order as below:

1. Feasibility study to conduct detailed research on the subject of running safety.
2. Conduct a stochastic comparison between running safety and passenger comfort to find the dominant design criteria.
3. Investigate the influence of soil-structure interaction.
4. Propose minimum design requirements for running safety.

5.2 Conclusions

The main conclusions that emerge from the attached papers are summarized below:

- Performing preliminary reliability evaluations on generic short to medium span bridges using the FORM revealed that applying a constant safety factor to all bridges with any conditions does not guarantee that they will all have an equivalent safety margin. It also highlighted the point that still the final design may violate the desired level of safety.
- The results of the FORM showed that the coach length, flexural rigidity, bridge geometry, and system damping are the most important variables in evaluating the running safety of high-speed railway bridges.
- It has been shown that both subset simulation and meta-model based MC using PCE can significantly reduce the computational cost of reliability assessment of railway bridges. Moreover, their computed failure probabilities agree well with the benchmark solution from crude MC.
- It has been proved by stochastic comparison between the limit states of running safety and passenger comfort that the former dominates the design almost in all conditions. It should be noted that the difference between these two performance functions decreases for shorter span bridges or trains passing at lower speeds.
- It was found that the use of the stacked model can significantly improve the performance of the weak models in the reliability evaluation of railway bridges. This conclusion is obtained by comparing the violation probability of the MC assisted by stacked classification-based meta-models with the crude MC for a wide range of operating speeds.
- It was found that neglecting SSI effects can result in an underestimated safety index for shorter span bridges; however, it is possible for the evaluated safety index of longer simply-supported bridges to be an overestimated value.
- It was shown that it would be possible to assure a consistent safety level for running safety limit state of bridges with different span lengths by neglecting the conventional safety factor of 2 and using minimum allowable mass per length or maximum permissible fundamental frequency obtained from reliability-based design optimization methods.

5.3 Further research

In this licentiate thesis, reliability-based assessment methods have been applied to investigate various aspects of running safety of high-speed railway bridges, and

5.3. FURTHER RESEARCH

the reliability-based design optimization approach used in a later step to propose minimum bridge design requirements. Some suggestions for possible future studies on this topic are given below.

- More bridges should be surveyed, especially those on high-speed lines, to obtain a more realistic feasible domain and to assign a more reliable probability distribution for the geometric properties of the bridge.
- The use of modification factors to implement effects of load distribution within ballast, rail irregularity, and train-track-bridge interaction can improve the performance of moving load models; however, these are still approximate methods. Complex finite element models should be constructed that explicitly account for these parameters.
- Discrete element models of the track can be constructed to numerically investigate the ballast destabilization problem. This will lead to a better understanding of the nature of this phenomenon. Also, a more reliable probability distribution for the vertical acceleration limit can be extracted.
- Updating the partial safety factor of the vertical acceleration limit seems to be the simplest possible modification of the conventional design approaches. It is easier to apply and well accepted in design practice. Therefore, it is recommended to aim for a uniform (consistent) safety factor in conjunction with the previous point.
- The concepts presented in this study are limited to ballasted bridges; however, similar concerns exist for non-ballasted bridges. Therefore, a systematic approach should be taken to investigate various aspects of this issue for such bridges and update existing partial safety factors.
- Consideration of the consequences of each failure mode is very important when updating design codes. Therefore, it is recommended to collect information about possible costs and implement them in the followed procedure of this study.

References

- Agarwal, H. and J. Renaud (2004). Reliability based design optimization using response surfaces in application to multidisciplinary systems. *Engineering Optimization* 36(3), 291–311.
- Akaike, H. (1974). A new look at the statistical model identification. *IEEE Transactions on Automatic Control* 19(6), 716–723.
- Akin, J. E. and M. Mofid (1989). Numerical solution for response of beams with moving mass. *Journal of Structural Engineering* 115(1), 120–131.
- Alizadeh, R., J. K. Allen, and F. Mistree (2020). Managing computational complexity using surrogate models: a critical review. *Research in Engineering Design* 31(3), 275–298.
- Allahvirdizadeh, R., A. Andersson, and R. Karoumi (2020). Reliability assessment of the dynamic behavior of high-speed railway bridges using first order reliability method. In *Eurodyn 2020, 11th International Conference on Structural Dynamics Athens, 23-26 November, 2020.*, Volume 2, pp. 3438–3450.
- Allahvirdizadeh, R., A. Andersson, and R. Karoumi (2021a). Minimum design requirements of high-speed railway bridges using reliability-based optimization. *Unpublished Manuscript*.
- Allahvirdizadeh, R., A. Andersson, and R. Karoumi (2021b). Surrogate-assisted versus subset simulation-based stochastic comparison between running safety and passenger comfort design criteria of high-speed railway bridges. In *ESREL 2021, 31st European Safety and Reliability Conference, 19-23 September, 2021*.
- Allahvirdizadeh, R., A. Andersson, and R. Karoumi (2022). Ensemble meta-models for running safety assessment of high-speed railway bridges considering soil-structure interaction effects. In *Eurodyn 2021-2022, 13th International Conference on Structural Safety and Reliability, 20-24 June, 2022*.
- Arvidsson, T. (2018). *Train–Track–Bridge Interaction for the Analysis of Railway Bridges and Train Running Safety*. Ph. D. thesis, KTH Royal Institute of Technology.
- Arvidsson, T. and R. Karoumi (2014). Train–bridge interaction—a review and discussion of key model parameters. *International Journal of Rail Transportation* 2(3), 147–186.
- Arvidsson, T., R. Karoumi, and C. Pacoste (2014). Statistical screening of modelling alternatives in train–bridge interaction systems. *Engineering Structures* 59, 693–701.

CHAPTER REFERENCES

- Au, S.-K. and J. L. Beck (2001). Estimation of small failure probabilities in high dimensions by subset simulation. *Probabilistic Engineering Mechanics* 16(4), 263–277.
- Au, S. K., J. Ching, and J. Beck (2007). Application of subset simulation methods to reliability benchmark problems. *Structural Safety* 29(3), 183–193.
- Ayre, R., G. Ford, and L. Jacobsen (1950). Transverse vibration of a two-span beam under action of a moving constant force.
- Ayyub, B. M. and C.-Y. Chia (1992). Generalized conditional expectation for structural reliability assessment. *Structural Safety* 11(2), 131–146.
- Ayyub, B. M. and A. Haldar (1984). Practical structural reliability techniques. *Journal of Structural Engineering* 110(8), 1707–1724.
- Basudhar, A. and S. Missoum (2010). An improved adaptive sampling scheme for the construction of explicit boundaries. *Structural and Multidisciplinary Optimization* 42(4), 517–529.
- Beachkofski, B. and R. Grandhi (2002). Improved distributed hypercube sampling. In *43rd AIAA/ASME/ASCE/AHS/ASC Structures, Structural Dynamics, and Materials Conference*, pp. 1274.
- Biggs, J. (1964). *Introduction to Structural Dynamics*. McGraw-Hill, New York, N.Y.
- Blatman, G. (2009). *Adaptive sparse polynomial chaos expansions for uncertainty propagation and sensitivity analysis*. Ph. D. thesis, Clermont-Ferrand II.
- Blatman, G. and B. Sudret (2011). Adaptive sparse polynomial chaos expansion based on least angle regression. *Journal of Computational Physics* 230(6), 2345–2367.
- Burns, J. (2009). Centroidal voronoi tessellations. ProjectArchive. Retrieved from Wightman College: <https://www.whitman.edu/mathematics/SeniorProjectArchive/2009/burns.pdf>.
- Calgaro, J.-A., M. Tschumi, and H. Gulvanessian (2010). *Designers’ Guide to Eurocode 1: Actions on Bridges: EN 1991-2, EN 1991-1-1, -1-3 TO-1-7 and EN 1990 Annex A2*. Thomas Telford Ltd.
- Cantero, D., T. Arvidsson, E. O’Brien, and R. Karoumi (2016). Train–track–bridge modelling and review of parameters. *Structure and Infrastructure Engineering* 12(9), 1051–1064.
- CEN (2003a). *EN 1991-2. Eurocode 1: Actions on Structures*. European Committee for Standardisation.

- CEN (2003b). *EN 1991-2. Eurocode 1: Actions on structures - Part 2: Traffic Loads on Bridges*. European Committee for Standardisation.
- Chen, X., T. Hasselman, D. Neill, X. Chen, T. Hasselman, and D. Neill (1997). Reliability based structural design optimization for practical applications. In *38th Structures, structural dynamics, and materials conference*, pp. 1403.
- Chen, Y. (1978). Dynamic analysis of continuous beams subjected to moving loads. *Journal of the Chinese Institute of Civil and Hydraulic Engineering* 5(2), 1–7.
- Cheng, G., L. Xu, and L. Jiang (2006). A sequential approximate programming strategy for reliability-based structural optimization. *Computers & Structures* 84(21), 1353–1367.
- Cheng, K. and Z. Lu (2020). Structural reliability analysis based on ensemble learning of surrogate models. *Structural Safety* 83, 101905.
- Cho, T., M.-K. Song, and D. H. Lee (2010). Reliability analysis for the uncertainties in vehicle and high-speed railway bridge system based on an improved response surface method for nonlinear limit states. *Nonlinear Dynamics* 59(1), 1–17.
- Claus, H. and W. Schiehlen (1998). Modeling and simulation of railway bogie structural vibrations. *Vehicle System Dynamics* 29(S1), 538–552.
- Cornell, C. A. (1969). A probability-based structural code. 66(12), 974–985.
- Der Kiureghian, A., Y. Zhang, and C.-C. Li (1994). Inverse reliability problem. *Journal of Engineering Mechanics* 120(5), 1154–1159.
- Ditlevsen, O. (1981). Principle of normal tail approximation. *Journal of the Engineering Mechanics Division* 107(6), 1191–1208.
- Dobry, R. and G. Gazetas (1986). Dynamic response of arbitrarily shaped foundations. *Journal of Geotechnical Engineering* 112(2), 109–135.
- Doménech, A., P. Museros, and M. Martínez-Rodrigo (2014). Influence of the vehicle model on the prediction of the maximum bending response of simply-supported bridges under high-speed railway traffic. *Engineering Structures* 72, 123–139.
- Du, J., H. Li, and Y. He (2017). The method of solving structural reliability with multiparameter correlation problem. *Mathematical Problems in Engineering* 2017.
- Dubourg, V., B. Sudret, and J.-M. Bourinet (2011). Reliability-based design optimization using kriging surrogates and subset simulation. *Structural and Multidisciplinary Optimization* 44(5), 673–690.

CHAPTER REFERENCES

- Dubourg, V., B. Sudret, and F. Deheeger (2013). Metamodel-based importance sampling for structural reliability analysis. *Probabilistic Engineering Mechanics* 33, 47–57.
- Dugush, Y. and M. Eisenberger (2002). Vibrations of non-uniform continuous beams under moving loads. *Journal of Sound and Vibration* 254(5), 911–926.
- Durante, F. and C. Sempi (2010). Copula theory: an introduction. In *Copula Theory and Its Applications*, pp. 3–31. Springer.
- Echard, B., N. Gayton, and M. Lemaire (2011). AK-MCS: an active learning reliability method combining kriging and monte carlo simulation. *Structural Safety* 33(2), 145–154.
- Enevoldsen, I. and J. D. Sørensen (1994). Reliability-based optimization in structural engineering. *Structural Safety* 15(3), 169–196.
- ERRI (1999). *ERRI D214: Rail bridge for speeds > 200 km/h. Final report. Part A: Synthesis of the Results of D214Research*. European Rail Research Institute.
- European Commission. Directorate General for Mobility (2010). *High-speed Europe: A Sustainable Link Between Citizens*. Office for Official Publications of the European Communities.
- Frangopol, D. M. (1985). Structural optimization using reliability concepts. *Journal of Structural Engineering* 111(11), 2288–2301.
- Frýba, L. (1996). *Dynamics of Railway Bridges*. Thomas Telford Publishing.
- Frýba, L. (2001). A rough assessment of railway bridges for high speed trains. *Engineering Structures* 23(5), 548–556.
- Frýba, L. (2013). *Vibration of Solids and Structures under Moving Loads*, Volume 1. Springer Science & Business Media.
- Garg, V. and R. Dukkipati (1984). *Dynamics of Railway Vehicle Systems*. Academic Press, New York, N.Y.
- Gbadeyan, J. and S. Oni (1995). Dynamic behaviour of beams and rectangular plates under moving loads. *Journal of Sound and Vibration* 182(5), 677–695.
- Givoni, M. (2007). Environmental benefits from mode substitution: Comparison of the environmental impact from aircraft and high-speed train operations. *International Journal of Sustainable Transportation* 1(4), 209–230.
- Goel, T., R. T. Haftka, W. Shyy, and N. V. Queipo (2007). Ensemble of surrogates. *Structural and Multidisciplinary Optimization* 33(3), 199–216.

- Hailin, W., O. Xunmin, and Z. Xiliang (2017). Mode, technology, energy consumption, and resulting co2 emissions in china’s transport sector up to 2050. *Energy Policy* 109, 719–733.
- Hammarling, S., C. J. Munro, and F. Tisseur (2013). An algorithm for the complete solution of quadratic eigenvalue problems. *ACM Transactions on Mathematical Software (TOMS)* 39(3), 1–19.
- Hasofer, A. M. and N. C. Lind (1974). Exact and invariant second-moment code format. *Journal of the Engineering Mechanics Division* 100(1), 111–121.
- Hillerborg, A. (1951). *Dynamic Influences of Smoothly Running Loads on Simply Supported Girders*. KTH Royal Institute of Technology, Stockholm.
- Hirzinger, B., C. Adam, M. Oberguggenberger, and P. Salcher (2020). Approaches for predicting the probability of failure of bridges subjected to high-speed trains. *Probabilistic Engineering Mechanics* 59, 103021.
- Hirzinger, B., C. Adam, P. Salcher, and M. Oberguggenberger (2019). On the optimal strategy of stochastic-based reliability assessment of railway bridges for high-speed trains. *Meccanica* 54(9), 1385–1402.
- Hull, T. E. and A. R. Dobell (1962). Random number generators. *SIAM Review* 4(3), 230–254.
- Hurtado, J. E. (2013). *Structural Reliability: Statistical Learning Perspectives*, Volume 17. Springer Science & Business Media.
- James, G., D. Witten, T. Hastie, and R. Tibshirani (2013). *An introduction to statistical learning*, Volume 112. Springer.
- Jeffcott, H. (1929). On the vibration of beams under the action of moving loads. *The London, Edinburgh, and Dublin Philosophical Magazine and Journal of Science* 8(48), 66–97.
- Jin, Z., B. Huang, J. Ren, and S. Pei (2018). Reduction of vehicle-induced vibration of railway bridges due to distribution of axle loads through track. *Shock and Vibration* 2018.
- Jones, D. R., M. Schonlau, and W. J. Welch (1998). Efficient global optimization of expensive black-box functions. *Journal of Global Optimization* 13(4), 455–492.
- Kahn, H. (1956). Use of different monte carlo sampling techniques,[in] proceedings of symposium on monte carlo methods,[ed.] ha meyer.
- Kanakasabai, P. and A. K. Dhingra (2014). Reliability-based design optimization with progressive surrogate models. *Engineering Optimization* 46(12), 1609–1627.

CHAPTER REFERENCES

- Kroetz, H. M., R. K. Tessari, and A. T. Beck (2017). Performance of global meta-modeling techniques in solution of structural reliability problems. *Advances in Engineering Software* 114, 394–404.
- Kumakura, T., H. Ishii, and T. Konishi (2010). Seismic assessment of ballasted tracks in large-scale earthquakes. *JR East Technical Review* 17.
- Labeyrie, J. (1997). Response surface methodology in structural reliability. In *Probabilistic Methods for Structural Design*, pp. 39–58. Springer.
- Lacaze, S. and S. Missoum (2014). A generalized max-min sample for surrogate update. *Structural and Multidisciplinary Optimization* 49(4), 683–687.
- Lind Östlund, J., A. Andersson, M. Ülker-Kaustell, and J.-M. Battini (2020). On the influence of shallow soil strata on the dynamic soil–structure interaction of simply supported high-speed railway bridges. *International Journal of Rail transportation*, 1–19.
- Liu, K., G. De Roeck, and G. Lombaert (2009). The effect of dynamic train–bridge interaction on the bridge response during a train passage. *Journal of Sound and Vibration* 325(1-2), 240–251.
- Liu, K., N. Zhang, H. Xia, and G. De Roeck (2014). A comparison of different solution algorithms for the numerical analysis of vehicle–bridge interaction. *International Journal of Structural Stability and Dynamics* 14(02), 1350065.
- Liu, P.-L. and A. Der Kiureghian (1986). Multivariate distribution models with prescribed marginals and covariances. *Probabilistic Engineering Mechanics* 1(2), 105–112.
- Lu, H. and Z. Zhu (2018). A method for estimating the reliability of structural systems with moment-matching and copula concept. *Mechanics Based Design of Structures and Machines* 46(2), 196–208.
- Madsen, H. O. (1988). Omission sensitivity factors. *Structural Safety* 5(1), 35–45.
- Madsen, H. O., S. Krenk, and N. C. Lind (2006). *Methods of Structural Safety*. Courier Corporation.
- Marelli, S. and B. Sudret (2014). Uqlab: A framework for uncertainty quantification in matlab. In *Vulnerability, uncertainty, and risk: quantification, mitigation, and management*, pp. 2554–2563.
- Melchers, R. (1984). Efficient monte-carlo probability integration. Technical Report Research Report No. 7/1984, Department of Civil Engineering, Monash University, Australia.
- Melchers, R. (1989). Importance sampling in structural systems. *Structural Safety* 6(1), 3–10.

- Melchers, R. E. and A. T. Beck (2018). *Structural Reliability Analysis and Prediction* (Third ed.). John Wiley & Sons.
- Missoum, S., S. Lacaze, E. Boroson, and P. Jiang (2015). CODES: Computational optimal design of engineering systems. <http://codes.arizona.edu/>.
- Moustapha, M. and B. Sudret (2019). Surrogate-assisted reliability-based design optimization: a survey and a unified modular framework. *Structural and Multidisciplinary Optimization*, 1–20.
- Museros, P., A. Andersson, V. Martí, and R. Karoumi (2021). Dynamic behaviour of bridges under critical articulated trains: Signature and bogie factor applied to the review of some regulations included in en 1991-2. *Proceedings of the Institution of Mechanical Engineers, Part F: Journal of Rail and Rapid Transit* 235(5), 655–675.
- Museros, P., M. Romero, A. Poy, and E. Alarcón (2002). Advances in the analysis of short span railway bridges for high-speed lines. *Computers & Structures* 80(27-30), 2121–2132.
- Myers, R. H., D. C. Montgomery, and C. M. Anderson-Cook (2016). *Response Surface Methodology: Process and Product Optimization Using Designed Experiments*. John Wiley & Sons.
- Nakamura, T., E. Sekine, and Y. Shirae (2011). Assessment of aseismic performance of ballasted track with large-scale shaking table tests. *Quarterly Report of RTRI* 52(3), 156–162.
- NIST (2012). Soil-structure interaction for building structures. *Report No. NIST GCR 12-917-21*.
- Nowak, A. S. and K. R. Collins (2012). *Reliability of Structures* (Second ed.). CRC Press.
- Papaefthymiou, G. and D. Kurowicka (2008). Using copulas for modeling stochastic dependence in power system uncertainty analysis. *IEEE Transactions on Power Systems* 24(1), 40–49.
- Rackwitz, R. and B. Flessler (1978). Structural reliability under combined random load sequences. *Computers & Structures* 9(5), 489–494.
- Ramu, P., X. Qu, B. D. Youn, R. T. Haftka, and K. K. Choi (2006). Inverse reliability measures and reliability-based design optimisation. *International Journal of Reliability and Safety* 1(1-2), 187–205.
- Rao, G. (2000). Linear dynamics of an elastic beam under moving loads. *Journal of Vibration and Acoustics* 122(3), 281–289.

CHAPTER REFERENCES

- Rasmussen, C. and C. Williams (2006). *Gaussian Processes for Machine Learning*. MIT Press: Cambridge, MA.
- Rocha, J., A. Henriques, and R. Calçada (2012). Safety assessment of a short span railway bridge for high-speed traffic using simulation techniques. *Engineering Structures* 40, 141–154.
- Rocha, J., A. Henriques, and R. Calçada (2014). Probabilistic safety assessment of a short span high-speed railway bridge. *Engineering Structures* 71, 99–111.
- Rocha, J., A. Henriques, R. Calçada, and A. Rönquist (2015). Efficient methodology for the probabilistic safety assessment of high-speed railway bridges. *Engineering Structures* 101, 138–149.
- Rocha, J. M., A. A. Henriques, and R. Calçada (2016). Probabilistic assessment of the train running safety on a short-span high-speed railway bridge. *Structure and Infrastructure Engineering* 12(1), 78–92.
- Rogers, S. and M. Girolami (2020). *A First Course in Machine Learning* (Second ed.). Chapman and Hall/CRC.
- Romero, A., M. Solís, J. Domínguez, and P. Galvín (2013). Soil–structure interaction in resonant railway bridges. *Soil Dynamics and Earthquake Engineering* 47, 108–116.
- Rosenblatt, M. (1952). Remarks on a multivariate transformation. *The Annals of Mathematical Statistics* 23(3), 470–472.
- Sadiku, S. and H. Leipholz (1987). On the dynamics of elastic systems with moving concentrated masses. *Ingenieur-Archiv* 57(3), 223–242.
- Sagi, O. and L. Rokach (2018). Ensemble learning: A survey. *Wiley Interdisciplinary Reviews: Data Mining and Knowledge Discovery* 8(4), e1249.
- Saka, Y., M. Gunzburger, and J. Burkardt (2007). Latinized, improved lhs, and cvt point sets in hypercubes. *International Journal of Numerical Analysis and Modeling* 4(3-4), 729–743.
- Salcher, P. and C. Adam (2020). Estimating exceedance probabilities of railway bridge vibrations in the presence of random rail irregularities. *International Journal of Structural Stability and Dynamics* 20(13), 2041005.
- Salcher, P., C. Adam, and A. Kuisle (2019). A stochastic view on the effect of random rail irregularities on railway bridge vibrations. *Structure and Infrastructure Engineering* 15(12), 1649–1664.
- Sammut, C. and G. I. Webb (2011). *Encyclopedia of Machine Learning*. Springer Science & Business Media.

REFERENCES

- Santner, T. J., B. J. Williams, W. I. Notz, and B. J. Williams (2003). *The Design and Analysis of Computer Experiments*, Volume 1. Springer.
- Schwarz, G. et al. (1978). Estimating the dimension of a model. *Annals of Statistics* 6(2), 461–464.
- Sørensen, J. D. (2011). *Notes in Structural Reliability Theory and Risk Analysis*. Aalborg University, Denmark.
- Speagle, J. S. (2019). A conceptual introduction to markov chain monte carlo methods. *ArXiv Preprint arXiv:1909.12313*.
- Sridharan, N. and M. AK (1979). Numerical analysis of vibration of beams subjected to moving loads. *Journal of Sound and Vibration* 65(1), 147–150.
- Stanišić, M. (1985). On a new theory of the dynamic behavior of the structures carrying moving masses. *Ingenieur-Archiv* 55(3), 176–185.
- Stanišić, M. M. and J. C. Hardin (1969). On the response of beams to an arbitrary number of concentrated moving masses. *Journal of the Franklin Institute* 287(2), 115–123.
- Stewart, J. P., G. L. Fenves, and R. B. Seed (1999). Seismic soil-structure interaction in buildings. i: Analytical methods. *Journal of Geotechnical and Geoenvironmental Engineering* 125(1), 26–37.
- Stokes, S. G. G. (1849). *Discussion of a Differential Equation Relating to the Breaking of Railway Bridges*. Printed at the Pitt Press by John W. Parker.
- Sudret, B. (2008). Global sensitivity analysis using polynomial chaos expansions. *Reliability Engineering & System Safety* 93(7), 964–979.
- Sudret, B. (2012). Meta-models for structural reliability and uncertainty quantification. *ArXiv Preprint arXiv:1203.2062*.
- Takemiya, H. and X. C. Bian (2007). Shinkansen high-speed train induced ground vibrations in view of viaduct-ground interaction. *Soil Dynamics and Earthquake Engineering* 27(6), 506–520.
- Teixeira, R., M. Nogal, and A. O’Connor (2021). Adaptive approaches in metamodel-based reliability analysis: A review. *Structural Safety* 89, 102019.
- Timoshenko, S. (1922). On the forced vibrations of bridges. *Philosophical Magazine and Journal of Science* 43(257), 1018–1019.
- Timoshenko, S. and D. Young (1955). *Vibration Problems in Engineering*. D. Van Nostrand, New York, N.Y.

CHAPTER REFERENCES

- Ting, E., J. Genin, and J. Ginsberg (1974). A general algorithm for moving mass problems. *Journal of Sound and Vibration* 33(1), 49–58.
- Tisseur, F. and K. Meerbergen (2001). The quadratic eigenvalue problem. *SIAM Review* 43(2), 235–286.
- Ülker-Kaustell, M., R. Karoumi, and C. Pacoste (2010). Simplified analysis of the dynamic soil–structure interaction of a portal frame railway bridge. *Engineering Structures* 32(11), 3692–3698.
- Vellozzi, J. (1967). Vibration of suspension bridges under moving loads. *Journal of the Structural Division* 93(4), 123–138.
- Wang, R. (2020). *Reliability-Based Fatigue Assessment of Existing Steel Bridges*. Licentiate Thesis, KTH Royal Institute of Technology.
- Wang, R.-T. (1997). Vibration of multi-span timoshenko beams to a moving force. *Journal of Sound and Vibration* 207(5), 731–742.
- Wu, J.-S. and C.-W. Dai (1987). Dynamic responses of multispan nonuniform beam due to moving loads. *Journal of Structural Engineering* 113(3), 458–474.
- Wu, Y. (2000). *Dynamic Interactions of Train-Rail-Bridge System Under Normal and Seismic Conditions*. Ph. D. thesis.
- Xia, H., N. Zhang, and W. Guo (2006). Analysis of resonance mechanism and conditions of train–bridge system. *Journal of Sound and Vibration* 297(3-5), 810–822.
- Xiu, D. and G. E. Karniadakis (2002). The wiener–askey polynomial chaos for stochastic differential equations. *SIAM Journal on Scientific Computing* 24(2), 619–644.
- Yang, F. and G. A. Fonder (1996). An iterative solution method for dynamic response of bridge–vehicles systems. *Earthquake Engineering & Structural Dynamics* 25(2), 195–215.
- Yang, Y. and J. Yau (1998). Vehicle-bridge interactions and applications to high speed rail bridges. In *Proceedings of the National Science Council, ROC*, Volume 22.
- Yang, Y.-B., J. Yau, Z. Yao, and Y. Wu (2004). *Vehicle-Bridge Interaction Dynamics: with Applications to High-speed Railways*. World Scientific.
- Yang, Y.-B., J.-D. Yau, and L.-C. Hsu (1997). Vibration of simple beams due to trains moving at high speeds. *Engineering Structures* 19(11), 936–944.

REFERENCES

- Yau, J., M. D. Martínez-Rodrigo, and A. Doménech (2019). An equivalent additional damping approach to assess vehicle-bridge interaction for train-induced vibration of short-span railway bridges. *Engineering Structures* 188, 469–479.
- Zacher, M. and M. Baessler (2005). Dynamic behaviour of ballast on railway bridges. *Dynamics of High-speed Railway Bridges* (978-0), 203–89540.
- Zangeneh Kamali, A. (2018). *Dynamic Soil-Structure Interaction of Railway Bridges: Numerical and Experimental Results*. Licentiate Thesis, KTH Royal Institute of Technology.
- Zangeneh Kamali, A., J.-M. Battini, C. Pacoste, and R. Karoumi (2019). Fundamental modal properties of simply supported railway bridges considering soil-structure interaction effects. *Soil Dynamics and Earthquake Engineering* 121, 212–218.
- Zangeneh Kamali, A., C. Svedholm, A. Andersson, C. Pacoste, and R. Karoumi (2018). Identification of soil-structure interaction effect in a portal frame railway bridge through full-scale dynamic testing. *Engineering Structures* 159, 299–309.
- Zhai, W., Z. Han, Z. Chen, L. Ling, and S. Zhu (2019). Train-track-bridge dynamic interaction: a state-of-the-art review. *Vehicle System Dynamics* 57(7), 984–1027.
- Zhai, W., H. Xia, C. Cai, M. Gao, X. Li, X. Guo, N. Zhang, and K. Wang (2013). High-speed train-track-bridge dynamic interactions—part i: theoretical model and numerical simulation. *International Journal of Rail Transportation* 1(1-2), 3–24.
- Zhang, N., H. Xia, W. Guo, and G. De Roeck (2010). A vehicle-bridge linear interaction model and its validation. *International Journal of Structural Stability and Dynamics* 10(02), 335–361.
- Zheng, D., Y. Cheung, F. Au, and Y. Cheng (1998). Vibration of multi-span non-uniform beams under moving loads by using modified beam vibration functions. *Journal of Sound and Vibration* 212(3), 455–467.

